A FINITE STRAIN THEORY, AND ITS APPLICATION TO THE PLANE STRESS RESPONSE OF POLYURETHANE

by

G. Sylvester Healy, B.S., M.S.

Thesis submitted to the Graduate Faculty of the
Virginia Polytechnic Institute
in candidacy for the degree of
DOCTOR OF PHILOSOPHY
in
Engineering Mechanics

APPROVED:

Chairman, T. S. Chang

D. Frederick

L. McFadden

F. J. Maher

H. L. Wood

May, 1966

Blacksburg, Virginia

TABLE OF CONTENTS

LIST OF FIGURES

LIST OF TABLES

I. INTRODUCTION

As the title of this thesis suggests, a finite strain theory is going to be proposed; the validity of the proposed theory will be checked by several examples for an elastomeric material. Finite strain is defined by Frederick and Chang[1]* to be: "...the strain that occurs in the medium when no restrictions are placed on the magnitude of displacements or derivatives of the displacement with respect to position. The latter are called displacement gradients."

A series of fundamental papers pertinent to the response of "rubber-like" material was published by Rivlin[2], [3], [4]. In his first paper, Rivlin[2] developed the general theory of large elastic deformations in the classical manner (after Love[5]) without utilizing any specific stress-strain relationship. He then considers a neo-Hookean** material and demonstrates its agreement with

---

* The numbers in parentheses refer to the list of cited literature contained in the Bibliography.

** A neo-Hookean material is a material where the elastic potential function can be developed as a function of the strain invariants.

statistical studies. Two techniques are used in the development of the equations of motion and the formulation of the boundary conditions i.e.: the stress-strain relations and the stored elastic energy for a given state of strain. (In other words, to specify the elastic properties of a material, one may either state an explicit potential function or state a stress-strain relationship.) Rivlin[2] then demonstrates that the results of these two techniques are equivalent. In his second paper, Rivlin[3] assumed that pure, homogeneous deformation yields the only possible equilibrium state for the body. The equilibrium states of a cuboid of incompressible, neo-Hookean material are studied under the action of uniform normal loads applied to the faces of the cuboid. The results of this paper indicated that if the stresses or loads are specified; a stable, unique equilibrium state exists for the body in question. Under other specified load conditions eight equilibrium states are possible. Five of these eight are unstable, with three being stable but not necessarily unique. This, in general, indicated that the equilibrium state of a body depends upon the order in which specified loads are applied. In the third paper, Rivlin[4] transformed the equations of motion and the boundary conditions from the Cartesian coordinates used in the first two papers

(Rivlin[2], [3]) into cylindrical coordinates. Assuming an incompressible, neo-Hookean material, Rivlin[4] studied the special cases of a simple torsion and a simple torsion coupled with a simple extension applied to a right circular cylinder and a right circular cylindrical tube.

In view of Rivlin's[2] first paper, the proposed theory will be formulated by assuming a specific stress-strain relationship. It is believed that it is easier to formulate the problem by specifying a stress-strain relationship than by developing an elastic potential function.

Several authors solve finite strain problems using the method of the elastic potential function. Green and Zerna[6], Murnaghan[7], Mooney[8], and Carmichael and Holdaway[9], [10] all attack the finite strain problem in the manner discussed by Rivlin[2] or in a very similar manner. Murnaghan[7] develops the large deformation theory by means of matrices and defines the elastic potential function in a manner similar to Rivlin[2]. The work of Mooney[8] and Carmichael and Holdaway[9], [10] is very similar to the work of Rivlin[2], the primary difference being in the form of the elastic potential function.

The examples that will be used to evaluate the validity of the proposed theory will be:

1. uniaxial compression

ii. uniaxial tension

iii. shear

iv. a specific problem involving a combined system of compression, tension and shear.

The specific problem of case iv. above will be the response of a clamped, hubbed, circular, elastomeric plate which is subjected to a finite, axi-symmetric rotation of the hub.

In the process of formulating and solving the specific problem of the response of the clamped, hubbed, circular plate to finite, axi-symmetric rotation of the hub; the equations describing the nonlinear response to finite strain uniaxial compression, uniaxial tension, and shear will also be developed.

The solution of a finite, circular plate subject to infinitesimal, axi-symmetric torsional deformation is well known. Timoshenko and Goodier[11] present the solution as an illustrative example. The method of solution used by Timoshenko and Goodier[11] is quite elementary, utilizing only the Equilibrium Equations. Consequently, their solution is in terms of stresses only. Prescott[12] mentions the problem in passing, as an illustration of a solution yielded by a particular, assumed stress function ($E\phi = -iH \log (re^{i\theta})$). Prescott[12] obtains the same

solution as Timoshenko and Goodier[10]. The problem proposed by Timoshenko and Goodier[10] concerns a couple applied to a disc which is balanced by a couple applied to the center of the disc. Prescott[11] defines his solution as yielding the "stresses that would be produced by tightening up a nut on a bolt passing through the plate if the plate resisted the applied couple."

A similar problem, the problem of the rotation of a hub in a stretched infinite membrane, is attacked by Stein and Hedgepeth[13]. The assumptions involved in their analysis are: "The membrane considered is elastic, isotropic, has no bending stiffness, and cannot carry compressive stress." In addition to this, they assume small average strains, uniform pre-stress and radial symmetry. Their method of attack is straightforward, utilizing the conventional elasticity approach. They obtain the solutions for the radial and transverse stresses, and then using Hooke's Law and the strain-displacement equations, they develop the solutions for the displacements.

The work of Stein and Hedgepeth[13] was extended by Mikulas[14] who solved the problem of the behavior of a finite, stretched membrane subjected to the assumptions used by Stein and Hedgepeth[13]. Mikulas[14] obtained closed form solutions for several boundary conditions and

presented his results as torque-rotation plots.

Gubkin[15] investigated the problem of an annular, circular plate with a central hub which is loaded by the rotation of the hub as an illustrative problem in the determination of optical anisotrophy in terms of viscous flow. In the process of his discussion, Gubkin[15] makes the following statements which are of interest:

i. "For any isotropic material in the presence of simple shear the maximums of the shearing stresses appeared to be concentric circles."

ii. "The trajectories of the principal stresses form two families of logarithmic spirals."

iii. "In view of this, the principal stresses are equal in value but opposite in sign."

However, these statements are made with respect to an infinitesimal, linear, elasticity analysis of the problem.

A related problem, the behavior of a right circular cylinder subjected to torsion is used as an illustrative example by Rivlin[4], Green and Zerna[6] and Murnaghan[7]. Murnaghan[7] discusses the problem quite thoroughly for the finite deformation case.

On the basis of the discussion given by Murnaghan[7] on the solution of the torsion of a right circular cylinder, the possibility of solving the problem of the clamped,

hubbed, elastomeric circular plate subjected to finite rotations of the hub by means of the elastic potential function using the methods of superposition was considered. However, in view of the results of Rivlin's[3] second paper (concerning superposition); it was decided that a superposition solution was not feasible.

As is obvious, a search of the literature did not yield any direct reference to the problem of the analysis of the behavior of a clamped, hubbed, elastomeric, circular plate subjected to finite rotation of the hub. Consequently, this problem will not be attempted. The analysis of the problem, which follows, will be attempted utilizing the proposed finite strain theory.

II. LIST OF SYMBOLS

A_1, A_2	plate parameters associated with the second approximation solution
B_o, B_1, B_2, B_3	plate parameters associated with the second approximation solution
C_o, C_1, C_2, C_3, $\cdots$, C_6	plate parameters associated with the third approximation solution
D_1, D_2, D_3, $\cdots$, D_9	plate parameters associated with the third approximation solution
E_{--}	components of the Eulerian, non-linear strain tensor
G	the infinitesimal shearing modulus of elasticity
G_{--}	components of the metric tensor in the deformed body
$\hat{G}_-$	a base vector along the - coordinate axis of a set of coordinate axes erected in the deformed body
T	the torque applied to the central hub of the circular plate
a	the inside radius of the circular plate
b	the outside radius of the circular plate
$c = (b/a)^2$	the ratio of the outside radius to the inside radius of the circular plate squared
$\hat{e}_-$	a unit vector along the - axis of an orthogonal polar coordinate system erected in the deformed body
g_{--}	components of the metric tensor in the undeformed body

$\vec{g}_-$	a covariant base vector along the - coordinate axis of a set of coordinate axes located in the undeformed body
h	the plate thickness
k	a material constant
p	the dimensionless "radial" displacement
p_0	a hub rotation parameter
p_1	the first approximation dimensionless "radial" displacement
p_2	the second approximation dimensionless "radial" displacement
p_3	the third approximation dimensionless "radial" displacement
q	the dimensionless "transverse" displacement
q_0	a hub rotation parameter
q_1	the first approximation dimensionless "transverse" displacement
q_2	the second approximation dimensionless "transverse" displacement
q_3	the third approximation dimensionless "transverse" displacement
r	the radial space coordinate
u	the "radial" displacement
v	the "transverse" displacement
$\vec{v}$	the displacement vector
w	the longitudinal displacement
$x = (b/r)^2$	a space transformation variable

y	a dummy space variable
z	the longitudinal space coordinate
ds_i	the component of an infinitesimal line element along the θ^i coordinate axis of a coordinate system located in the deformed body
$(ds_i)_o$	the length of the preceding component of an infinitesimal line element before deformation
$\alpha_{\_\_}$	the angle between two coordinate axes before deformation
$\beta_{\_\_}$	the angle between the above two coordinate axes after deformation
ϵ_{ij}	the components of the physical normal strain if $i = j$ and the components of the physical shearing strain if $i \neq j$
θ	the polar angle in a polar two space or a cylindrical three space
θ^-	the - coordinate axis
μ	Poisson's ratio
$\sigma_{\_\_}$	the components of the stress tensor
ϕ	the plate loading parameter
ψ	the angular rotation of the rigid, central hub of the elastomeric, circular plate

III. THE INVESTIGATION

A.) OBJECT:

The object of the investigation is to propose and verify a rational method of attack upon a specific problem that can be classified as a finite strain problem. The method of attack will be developed in accordance with the conventional methods of linear Elasticity with two exceptions. The two exceptions will be that the strain displacement relations will be nonlinear, and will be expressed in the Eulerian form, and that a more general stress-strain relationship will be used instead of the conventional Hookean form.

B.) THE DEVELOPMENT OF THE GOVERNING EQUATIONS FOR THE SPECIFIC PROBLEM, AND THE STATEMENT OF THE FINITE STRAIN THEORY:

As was stated in the introduction, the specific problem that will be solved is the analysis of the behavior of a clamped, hubbed, circular, elastomeric plate when the hub is subjected to a finite rotation. Figure 1 shows a photograph of the plate.

The problem will be attacked as a generalized plane stress problem. Recall that the generalized plane stress problem is defined in the theory of linear Elasticity as a problem involving a body whose thickness is small; the body is loaded parallel to its faces; and, in addition, there are no deflections in the direction of the thickness. Five components of the stress tensor, namely, σ_{zz}, σ_{xz}, σ_{yz}, σ_{zx} and σ_{zy} (z in the direction of the thickness) are assumed to be zero on the unloaded faces of the body. Note that this does not imply that these stresses are zero throughout the body. However, if the thickness of the body is small, these stresses can be considered to be very small within the body; consequently, these stresses are considered to be zero at all points of the body. Moreover, the assumption that σ_{zz} is zero does not imply that ϵ_{zz}, the strain in the direction of the thickness, is zero. As a matter of fact, ϵ_{zz} is not

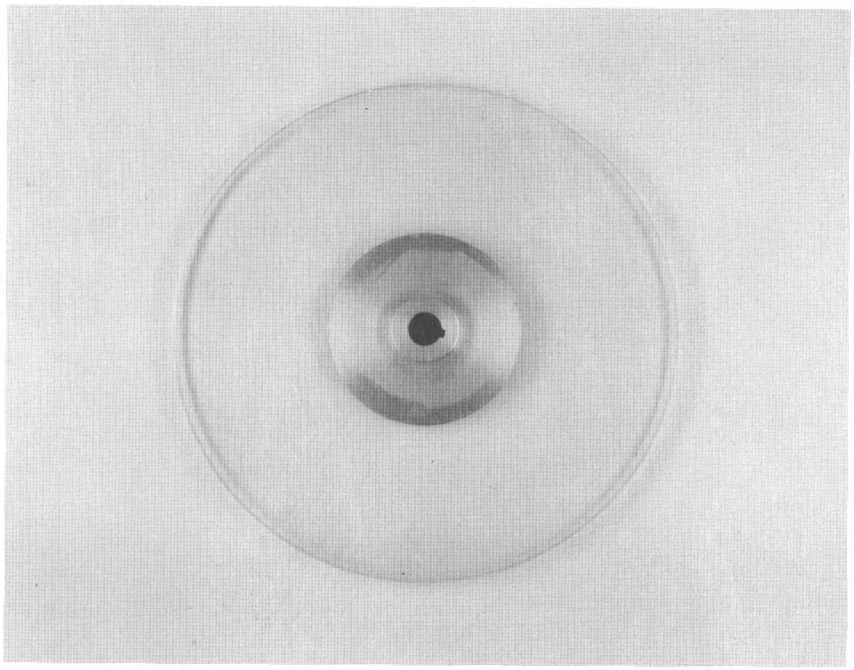

FIGURE 1 THE PLATE

zero as it represents the deformation in the direction of the thickness that is caused by the stresses σ_{xx} and σ_{yy} which act in the planes normal to the thickness. The deformation caused by ε_{zz} will be very small due to the small thickness of the body.

The specific problem to be solved is axi-symmetric for small rotations of the rigid, central hub. However, a question arose concerning the axi-symmetry when the rotation of the rigid, central hub became "large". It was thought that the plate might become unstable; and, consequently, suffer out-of-plane bending. (This, of course, would violate the generalized plane stress assumption.) To answer these questions, a polyurethane plate with an aluminum central hub was fabricated. The rigid central hub was then rotated about thirty degrees. The plate was checked photoelastically for symmetry of stress, and for all practical purposes the axi-symmetry property of the plate response was preserved for "large" angular rotations of the hub (see Figure 2). No out-of-plane response was noted. Consequently, no violations of the generalized plane stress assumptions are apparent.

The equations of equilibrium for an arbitrary element of a cylindrical body are easily developed, and are given in most standard texts in cylindrical coordinates. The equa-

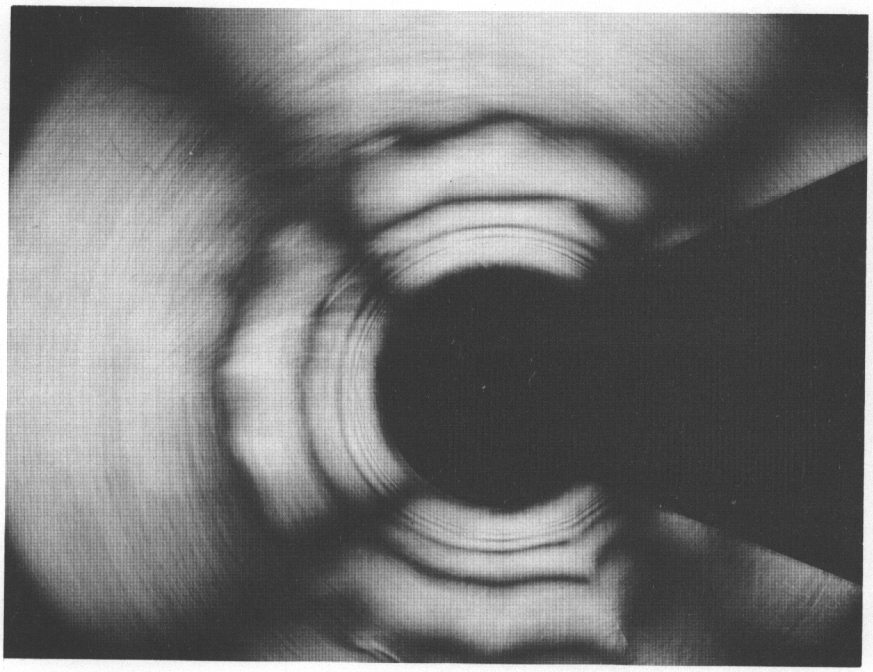

FIGURE 2 PHOTOELASTIC BASIS OF THE SYMMETRY ASSUMPTION

tions of equilibrium for an arbitrary element of a cylindrical body, in cylindrical coordinates are:

$$\sigma_{rr,r} + \frac{1}{r}\sigma_{r\theta,\theta} + \sigma_{rz,z} + \frac{\sigma_{rr} - \sigma_{\theta\theta}}{r} = 0 \qquad (1)$$

$$\sigma_{r\theta,r} + \frac{1}{r}\sigma_{\theta\theta,\theta} + \sigma_{\theta z,z} + \frac{2\sigma_{r\theta}}{r} = 0 \qquad (2)$$

$$\sigma_{rz,r} + \frac{1}{r}\sigma_{\theta z,\theta} + \sigma_{zz,z} + \frac{\sigma_{rz}}{r} = 0 \qquad (3)$$

In equations (1), (2) and (3), σ_{rr}, $\sigma_{r\theta}$, σ_{rz}, $\sigma_{\theta\theta}$, $\sigma_{\theta z}$ and σ_{zz} are the components of the stress tensor expressed in cylindrical coordinates; r is the radial space coordinate, θ is the polar angle and z is the longitudinal space coordinate. The comma in the subscript indicates that differentiation is performed with respect to the variable or variables following the comma; for example, $\sigma_{rr,r}$ means the first derivative of the radial, normal stress with respect to the radial space coordinate.

The strain-displacement relations will be formulated in the Eulerian manner as the effect of finite strain will be considered (see Sokolnikoff[16], pages 29-33). The Eulerian, nonlinear, strain tensor expressed in Cartesian coordinates is (see Frederick and Chang[1], page 82, equation 3.51)

$$E_{ij} = \frac{1}{2}\left[\frac{\partial u_i}{\partial y_j} + \frac{\partial u_j}{\partial y_i} - \frac{\partial u_r}{\partial y_i}\frac{\partial u_r}{\partial y_j}\right] \qquad (4)$$

where E_{ij} are the components of the Eulerian, nonlinear,

strain tensor; u_i, u_j and u_r are the displacement components associated with the i, j and r space coordinates; and i and j are range symbols whereas r is a summation symbol.

In terms of cylindrical coordinates we may write the components of the Eulerian, nonlinear strain tensor as:

$$E_{rr} = u_{,r} - \frac{1}{2}\left[(u_{,r})^2 + (v_{,r})^2 + (w_{,r})^2\right] \tag{4a}$$

$$E_{\theta\theta} = \frac{v_{,\theta} + u}{r} - \frac{1}{2r^2}\left[(u_{,\theta} - v)^2 + (v_{,\theta} + u)^2 + (w_{,\theta})^2\right] \tag{4b}$$

$$E_{zz} = w_{,z} - \frac{1}{2}\left[(u_{,z})^2 + (v_{,z})^2 + (w_{,z})^2\right] \tag{4c}$$

$$E_{r\theta} = \frac{1}{2}\left[\frac{u_{,\theta} - v}{r} + v_{,r}\right] - \frac{1}{2r}\left[u_{,r}\,(u_{,\theta} - v) + v_{,r}\,(v_{,\theta} + u) + w_{,r}\,(w_{,\theta})\right] \tag{4d}$$

$$E_{\theta z} = \frac{1}{2}\left[\frac{w_{,\theta}}{r} + v_{,z}\right] - \frac{1}{2r}\left[u_{,z}\,(u_{,\theta} - v) + v_{,z}\,(v_{,\theta} + u) + w_{,z}\,(w_{,\theta})\right] \tag{4e}$$

$$E_{rz} = \frac{1}{2}\left[u_{,z} + w_{,r}\right] - \frac{1}{2}\left[u_{,z}\,u_{,r} + v_{,z}\,v_{,r} + w_{,z}\,w_{,r}\right] \tag{4f}$$

In equations (4a) through (4f), E_{rr}, $E_{\theta\theta}$, $\cdots$ etc. are the Eulerian, nonlinear strain components in cylindrical coordinates; r, θ and z are the cylindrical space coordi-

nates previously defined; u, v and w are the displacements associated with the radial, polar angle, and longitudinal directions, respectively. The comma, again, denotes differentiation as previously explained. It should be emphasized, at this point, that these components of the Eulerian, nonlinear, strain tensor are developed with respect to the unit vectors of a cylindrical coordinate system located in the deformed body. In addition, it should be strongly emphasized that these components of the Eulerian, nonlinear strain tensor have physical meaning; but not in the conventional sense. For example, E_{rr} does not have the conventional meaning of a normal strain, and $E_{r\theta}$ does not have the conventional meaning of a shearing strain. However, the relationship between the components of the Eulerian, nonlinear strain tensor and the strain components based on the fundamental definitions of strain as enunciated in the linear Theory of Elasticity are easily developed, as will be demonstrated later.

Now, let us invoke the generalized plane stress assumption and the axi-symmetry assumption. If we apply these assumptions to the equilibrium equations, equations (1), (2) and (3), the following two equations result:

$$\sigma_{rr,r} + \frac{1}{r}(\sigma_{rr} - \sigma_{\theta\theta}) = 0 \qquad (1')$$

and

$$\sigma_{r\theta,r} + \frac{2}{r}\sigma_{r\theta} = 0 \qquad (2')$$

Equation (3) vanishes.

When the above assumptions are applied to the components of the Eulerian, nonlinear, strain tensor, equations (4a) to (4f), the following relationships arise:

$$E_{rr} = u_{,r} - \frac{1}{2}\left[(u_{,r})^2 + (v_{,r})^2\right] \qquad (5)$$

$$E_{r\theta} = \frac{1}{2}\left[v_{,r}\left(1 - \frac{u}{r}\right) + \frac{v}{r}(u_{,r} - 1)\right] \qquad (6)$$

$$E_{\theta\theta} = \frac{u}{r} - \frac{1}{2r^2}\left[u^2 + v^2\right] \qquad (7)$$

The other components vanish.

Now assume that a linear relationship exists between the components of the stress tensor of a polar two-space and the corresponding components of the Eulerian, nonlinear strain tensor. This assumption will then allow us to express the stress-strain relationships in the following manner:

$$\sigma_{rr} = \frac{2G}{1 - \mu}\left[E_{rr} + \mu E_{\theta\theta}\right] \qquad (8)$$

$$\sigma_{r\theta} = 2G E_{r\theta} \qquad (9)$$

$$\sigma_{\theta\theta} = \frac{2G}{1 - \mu}\left[E_{\theta\theta} + \mu E_{rr}\right] \qquad (10)$$

Using equations (8), (9) and (10), it can be shown that the strain energy is positive definite for a real material if G and $(1 + \mu)/(1 - \mu)$ are positive constants.

Note, that if the displacement gradients are small, the components of the Eulerian, nonlinear strain tensor will reduce to the conventional, linear strain components. Consequently, G must be the infinitesimal shearing modulus and μ must be equal to the value of Poisson's ratio as determined from the infinitesimal values of the shearing modulus and the elastic modulus.

Equations (8), (9) and (10) are the statements of the proposed finite strain theory. The theory may be stated, semantically, as follows:

> In the case of a finite strain problem, the components of the stress tensor are related to the components of the Eulerian, nonlinear strain tensor in exactly the same manner as the components of the stress tensor are related to the components of the linear strain tensor in the case of a linear strain problem. In addition, the material properties are identical to the infinitesimal material properties and the material properties are related as defined by the linear theory.

If equations (8), (9) and (10) are appropriately substituted into equations (1') and (2') the equilibrium equations for a thin circular plate are obtained in terms of the nonlinear Eulerian strain components. The resulting

equilibrium equations are:

$$E_{rr,r} + \mu E_{\theta\theta,r} + \frac{1-\mu}{r}(E_{rr} - E_{\theta\theta}) = 0 \qquad (11)$$

and

$$E_{r\theta,r} + \frac{2}{r} E_{r\theta} = 0 \qquad (12)$$

Substituting equations (5), (6) and (7) into equations (11) and (12) will yield the governing equations of the problem in terms of the displacements. The resulting governing equations are:

$$ru_{,rr} + u_{,r} - \frac{u}{r} - \Big[ru_{,r}\, u_{,rr} + \frac{\mu}{r} uu_{,r} + \frac{1-\mu}{2}(u_{,r})^2 - \Big(\frac{1+\mu}{2}\Big)\frac{u^2}{r^2} + rv_{,r}\, v_{,rr} + \frac{\mu}{r} vv_{,r} + \frac{1-\mu}{2}(v_{,r})^2 - \Big(\frac{1+\mu}{2}\Big)\frac{v^2}{r^2}\Big] = 0 \qquad (13)$$

and

$$u_{,rr}\Big(\frac{v}{r}\Big) + u_{,r}\Big(\frac{v}{r^2}\Big) - \Big(\frac{u}{r^2}\Big) v_{,r} + v_{,rr}\Big(1 - \frac{u}{r}\Big) + \frac{v_{,r}}{r} - \frac{v}{r^2} = 0 \qquad (14)$$

The governing equations, equations (13) and (14) are two, highly nonlinear, coupled, ordinary differential equations which must be solved, subject to the proper boundary conditions, to obtain a solution for the behavior of a clamped, hubbed, circular, elastomeric plate when the hub is subjected to a finite rotation.

An exact solution of equations (13) and (14) appears to be impossible at present, but a system of approximate solutions will be attempted. However, before any solution can be attempted, the boundary conditions of the problem must be established.

C.) THE BOUNDARY CONDITIONS:

Consider a circular plate of radius b which has a rigid, circular, central hub of radius a (see Figure 3). As the rigid central hub is twisted through an angle ϕ, a point which was originally at P moves along the arc PP' to a new position P'. The displacement of the point P as it moves from P to P' is represented by the displacement vector $\vec{v}$ which can be resolved at point P' in the following manner:

$$\vec{v} = v\,\vec{e}_\theta + u\,\vec{e}_r \tag{15}$$

where v is the magnitude of the displacement in the transverse direction at P' and u is the magnitude of the radial displacement at P', $\vec{e}_\theta$ and $\vec{e}_r$ are the unit vectors of an orthogonal polar coordinate system. Note, however, that v and u are the magnitudes of the components of the displacement vector, $\vec{v}$, in the directions of $\vec{e}_\theta$ and $\vec{e}_r$. Consequently, we may write:

$$v = a \sin \phi \tag{16}$$

$$u = a\,(1 - \cos \phi) \tag{17}$$

Equations (16) and (17) are the boundary conditions that must be satisfied at the boundary of the rigid, circular, central hub.

Now consider the point R, located on the outer boundary of the circular plate. The point R is rigidly fixed

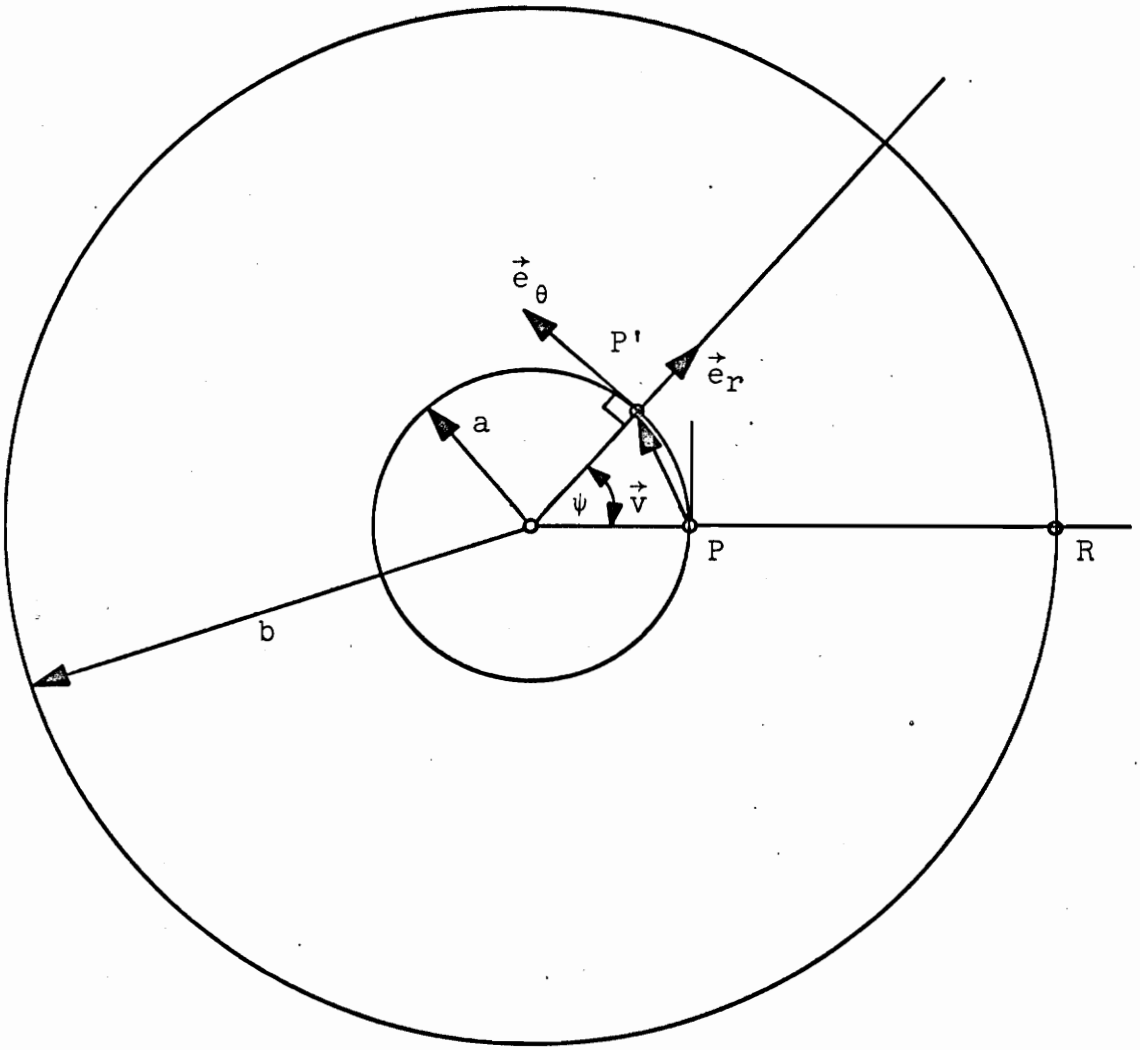

FIGURE 3

VISUAL INTERPRETATION OF THE BOUNDARY CONDITIONS OF THE HUBBED, CIRCULAR PLATE

and cannot suffer any displacement whatsoever. Therefore, the boundary conditions to be satisfied at the outer boundary of the plate are:

$$v = 0 \tag{18}$$

$$u = 0 \tag{19}$$

The boundary conditions to be satisfied by the solutions of equations (13) and (14) are then:

$$u = a(1 - \cos\phi) \quad \text{when } r = a \tag{20}$$

$$v = a \sin\phi \quad \text{when } r = a \tag{21}$$

and

$$u = 0 \quad \text{when } r = b \tag{22}$$

$$v = 0 \quad \text{when } r = b \tag{23}$$

D.) SIMPLIFICATION OF THE GOVERNING EQUATIONS AND THE BOUNDARY CONDITIONS:

Let us now make the following changes of variable:

$$p = \frac{u}{r} \tag{24}$$

$$q = \frac{v}{r} \tag{25}$$

$$x = \left(\frac{b}{r}\right)^2 \tag{26}$$

The above changes in variable reduce the governing equations, equations (13) and (14), to the forms:

$$p'' = p''p - x\frac{d}{dx}(p')^2 + q''q - x\frac{d}{dx}(q')^2 - k(p')^2 - k(q')^2 \tag{27}$$

and

$$q'' = pq'' - qp'' \tag{28}$$

In equations (27) and (28) p, q and x are as defined in equations (24), (25) and (26) and the prime indicates differentiation with respect to x. In equations (27), k is defined as follows:

$$k = \frac{1 + \mu}{2} \tag{29}$$

and μ is as defined following equation (10).

The boundary conditions, equations (20), (21), (22) and (23) are also simplified by the changes of variable given by equations (24), (25) and (26). The boundary conditions which arise due to the changes in variable are:

$$p = 1 - \cos \psi \qquad \text{when } x = \left(\frac{b}{a}\right)^2 \tag{30}$$

$$q = \sin \psi \qquad \text{when } x = \left(\frac{b}{a}\right)^2 \tag{31}$$

and

$$p = 0 \qquad \text{when } x = 1 \tag{32}$$

$$q = 0 \qquad \text{when } x = 1 \tag{33}$$

E.) SOLUTION OF THE GOVERNING EQUATIONS:

Equations (27) and (28) can be solved, approximately, using an iteration technique as follows:

1.) The First Approximation:

If the nonlinear terms of equations (27) and (28) are neglected, the following relationships arise:

$$p'' = 0 \qquad (27a)$$

and

$$q'' = 0 \qquad (28a)$$

These equations (equations (27a) and (28a)) can be regarded as the governing equations for the first approximations of p and q. Let us denote the first approximation of p by p_1, then, from equation (27a):

$$p_1'' = 0 \qquad (34)$$

and the corresponding boundary conditions are:

$$p_1 = 0 \qquad \text{when } x = 1 \qquad (32')$$

$$p_1 = 1 - \cos\phi = p_o \qquad \text{when } x = c = \left(\frac{b}{a}\right)^2 \qquad (30')$$

The form of the first approximation solution for p is:

$$p_1 = \left[1 - \cos\phi\right] \frac{x - 1}{c - 1} = p_o \frac{x - 1}{c - 1}$$

$$\text{where } p_o = 1 - \cos\phi \qquad (35)$$

Now, let the first approximation of q be q_1, then:

$$q_1'' = 0 \qquad (36)$$

Equation (36) was solved and subjected to the boundary conditions:

$$q_1 = 0 \qquad \text{when } x = 1 \tag{33'}$$

and

$$q_1 = \sin \psi = q_o \qquad \text{when } x = c$$

$$\text{where } c = \left(\frac{b}{a}\right)^2 \tag{31'}$$

The form of the first approximation solution for q is then:

$$q_1 = \left[\sin \psi\right] \frac{x - 1}{c - 1} = q_o \frac{x - 1}{c - 1}$$

$$\text{where } q_o = \sin \psi \tag{37}$$

The above solutions for p_1 and q_1 (equations (35) and (37)) are in agreement with the elementary solutions proposed by Stein and Hedgepeth[12] and Mikulas[13].

2.) The Second Approximation:

Let us now substitute p_1 and q_1 on the right hand side of equation (27); and thus obtain the equation to be solved for the second approximation of p. Consequently,

$$p_2'' = - \frac{k}{(c - 1)^2} \left[p_o^2 + q_o^2\right] \tag{38}$$

Solving this equation, subjected to the boundary conditions as given by equations (30') and (32') yields the second approximation solution for p in the following form:

$$p_2 = A_1 \frac{x - 1}{c - 1} + A_2 \frac{x^2 - 1}{(c - 1)^2} \tag{39}$$

where

$$A_1 = (1 - \cos \psi) \left[1 + k \frac{(c^2 - 1)}{(c - 1)^2}\right] \tag{40}$$

$$A_2 = - k (1 - \cos \phi) \tag{41}$$

Now, using the first approximation solution for q (equation (37)) and the second approximation solution for p (equation (39)); and appropriately substituting into equation (28) yields the equation to be solved for the second approximation of q:

$$q_2'' = \frac{k\, q_o\, (p_o^2 + q_o^2)\, (x - 1)}{(c - 1)^3} \tag{42}$$

Solving this equation, subject to the boundary conditions given by equations (31') and (33') yields the second approximation solution for q as follows:

$$q_2 = B_1 \frac{x - 1}{c - 1} + B_2 \frac{x^2 - 1}{(c - 1)^2} + B_3 \frac{x^3 - 1}{(c - 1)^3} \tag{43}$$

where

$$B_2 = - \frac{k \sin \phi\, (1 - \cos \phi)}{(c - 1)} \tag{44}$$

$$B_3 = \frac{1}{3} k \sin \phi\, (1 - \cos \phi) \tag{45}$$

$$B_1 = \sin \phi - B_2 \frac{c^2 - 1}{(c - 1)^2} - B_3 \frac{c^3 - 1}{(c - 1)^3} \tag{46}$$

3.) The Third Approximation:

Appropriately substituting the second approximations for p and q into equation (27) yields the governing equation to be solved for the third approximation of p. The equation to be solved is:

$$p_3'' = \left[- \frac{k(A_1^2 + B_1^2)}{(c-1)^2} - \frac{2(A_1A_2 + B_1B_2)}{(c-1)^3} - \frac{2(A_2^2 + B_2^2)}{(c-1)^4} - \frac{2B_2B_3}{(c-1)^5} \right]$$

$$+ \left[- \frac{2(1+2k)(A_1A_2 + B_1B_2)}{(c-1)^3} + \frac{6B_1B_3}{(c-1)^4} + \frac{6B_2B_3}{(c-1)^5} + \frac{6B_2^2}{(c-1)^6} \right] x$$

$$+ \left[- \frac{2(3+2k)(A_2^2 + B_2^2)}{(c-1)^4} - \frac{6(1+k)\,B_1B_3}{(c-1)^4} \right] x^2$$

$$- \left[\frac{2(7+3k)\,B_2B_3}{(c-1)^5} \right] x^3 - \left[\frac{3(10+3k)\,B_3^2}{(c-1)^6} \right] x^4 \qquad (47)$$

Now define the following parameters:

$$C_2 = -\frac{k}{2}(A_1^2 + B_1^2) - \frac{(A_1A_2 + B_1B_2)}{(c-1)} - \frac{(A_2^2 + B_2^2)}{(c-1)^2} - \frac{B_2B_3}{(c-1)^3} \qquad (48)$$

$$C_3 = -\frac{1}{3}(1+2k)(A_1A_2 + B_1B_2) + \frac{B_1B_3}{(c-1)} + \frac{B_2B_3}{(c-1)^2} + \frac{B_2^2}{(c-1)^3} \qquad (49)$$

$$C_4 = -\frac{1}{6}(3+2k)(A_2^2 + B_2^2) - \frac{1}{2}(1+k)\,B_1B_3 \qquad (50)$$

$$C_5 = -\frac{1}{10}(7+3k)\,B_2B_3 \qquad (51)$$

$$C_6 = -\frac{1}{10}(10+3k)\,B_3^2 \qquad (52)$$

$$C_1 = (1 - \cos\phi) - \sum_{n=2}^{6} C_n \frac{c^n - 1}{(c-1)^n} \qquad (53)$$

where the A_i and B_i are as previously defined.

Utilizing the above parameters the solution for the third approximation of p, subjected to the boundary conditions of equations (30') and (32'), is of the form:

$$p_3 = \sum_{n=1}^{6} C_n \frac{x^n - 1}{(c-1)^n} \tag{54}$$

Now let us substitute the third approximation for p and the second approximation for q into equation (28) to obtain the governing equation for the third approximation of q. The resulting governing equation is:

$$\begin{aligned} q_3'' = {} & \frac{2B_2C_0 - 2B_0C_2}{(c-1)^2} \\ & + \left[\frac{2B_2C_1 + 6B_3C_0 - 2B_1C_2 - 6C_3B_0}{(c-1)^3}\right] x \\ & + \left[\frac{6B_3C_1 - 6C_3B_1 - 12B_0C_4}{(c-1)^4}\right] x^2 \\ & + \left[\frac{4B_3C_2 - 4B_2C_3 - 20C_5B_0 - 12B_1C_4}{(c-1)^5}\right] x^3 \\ & + \left[\frac{-10C_4B_2 - 30C_5B_0 - 20C_5B_1}{(c-1)^6}\right] x^4 \\ & + \left[\frac{-18B_2C_3 - 6C_4B_3 - 30C_6B_1}{(c-1)^7}\right] x^5 \\ & + \left[\frac{-28B_2C_6 - 14B_3C_5}{(c-1)^8}\right] x^6 \\ & + \left[-\frac{24B_3C_6}{(c-1)^9}\right] x^7 \end{aligned} \tag{55}$$

Again, let us define a set of parameters as follows:

$$D_2 = \frac{1}{1.2}\left[2B_2C_0 - 2B_0C_2\right] \tag{56}$$

$$D_3 = \frac{1}{2.3}\left[2\,B_2C_1 + 6\,B_3C_0 - 2\,B_1C_2 - 6\,B_0C_3\right] \tag{57}$$

$$D_4 = \frac{1}{3.4}\left[6\,B_3C_1 - 6\,B_1C_3 - 12\,B_0C_4\right] \tag{58}$$

$$D_5 = \frac{1}{4.5}\left[4\,B_3C_2 - 4\,B_2C_3 - 20\,B_0C_5 - 12\,B_1C_4\right] \tag{59}$$

$$D_6 = \frac{1}{5.6}\left[-10\,B_2C_4 - 30\,B_0C_6 - 20\,B_1C_5\right] \tag{60}$$

$$D_7 = \frac{1}{6.7}\left[-18\,B_2C_5 - 6\,B_3C_4 - 30\,B_1C_6\right] \tag{61}$$

$$D_8 = \frac{1}{7.8}\left[-28\,B_2C_6 - 14\,B_3C_5\right] \tag{62}$$

$$D_9 = \frac{1}{8.9}\left[-24\,B_3C_6\right] \tag{63}$$

and

$$D_1 = \sin\phi - \sum_{n=2}^{9} D_n \frac{c^n - 1}{(c-1)^n} \tag{64}$$

where

$$B_0 = -\sum_{n=1}^{3} B_n\,(c-1)^{-n} \tag{65}$$

$$C_0 = -\sum_{n=1}^{6} C_n\,(c-1)^{-n} \tag{66}$$

and all other B_i and C_i are as previously defined.

Consequently, the third approximation solution for q subjected to the boundary conditions of equations (31') and (33') can be written in the form:

$$q_3 = \sum_{n=1}^{9} D_n \frac{x^n - 1}{(c - 1)^n} \tag{67}$$

Obviously, this method may be continued ad infinitum; however, the algebra involved in the analysis becomes extremely lengthy as is evidenced by the algebraic complexity of the constants D_1, D_2, $\cdots$, D_9 and C_1, C_2, $\cdots$, C_6 in the third approximation. If the method is extended, the solutions would be similar to equations (54) and (67) with a different range on n and, of course, the constants C_n and D_n would be different. The second and third approximations for p and q were programmed and checked on a Univac 1107 digital computer for comparison purposes. The deviation between the second and third approximation solutions of p and q was quite small. As a matter of fact, it is believed that the second approximation solutions of p and q are accurate enough for most engineering applications.

F.) COMPLETION OF THE SOLUTION:

Let us now consider equation (6), (9), (24), (25) and (26). Using equations (24), (25) and (26), transform the variables in equation (6) and substitute into equation (9). The result will be:

$$\sigma_{r\theta} = G \left[2x (p - 1) q' - 2xqp'\right] \tag{68}$$

Now, assume that the applied torque is resisted by circumferential shear, that is:

$$T = - 2 \sigma_{r\theta} \pi r^2 h \tag{69}$$

In equation (69), T is the applied torque, $\sigma_{r\theta}$ is the circumferential shearing stress, r is the radius of the arbitrary circumference, and h is the thickness of the plate.

Again, using equation (26) and equation (68); equation (69) is reexpressible as:

$$\frac{T}{4\pi hb^2 G} = (1 - p) q' + qp' \tag{70}$$

Equation (28) may be rewritten as:

$$(1 - p) q'' + qp'' = 0 \tag{28'}$$

or

$$\frac{d}{dx} (q' + qp' - pq') = 0 \tag{71}$$

Formally integrating equation (71) yields

$$(1 - p) q' + qp' = \text{a constant} \tag{72}$$

Comparing equations (70) and (72) we see that equations

(70) and (28) are equivalent.

Let

$$\frac{T}{4\pi hb^2G} = \phi \tag{73}$$

where ϕ is a loading parameter, and reexpress equations (70) and (72) as

$$(1 - p)\, q' + qp' = \phi \tag{74}$$

Equation (74) is the equation that relates the rotation of the hub to the applied torque.

We are now in a position to complete the solution of the problem using the third approximation solutions for p and q. To continue, let us reexpress equations (27) and (28) in equivalent form:

$$(1 + 2xp' - p)p'' + k\,(p')^2 + (2xq' - q)\, q'' + k\,(q')^2 = 0 \tag{27'}$$

$$(1 - p)\, q'' + qp'' = 0 \tag{28'}$$

Using a Univac 1107 digital computer the solution is completed in the following manner. In the following discussion k, equation (29), is assumed to be 0.75. This means that the material constant, μ, defined after equation (10) is assumed to be 0.5. In addition, let us assume that the plate to be analyzed is of a specific size. For this particular problem, assume a circular plate ten inches in diameter with a two inch diameter, rigid, circular hub and

a uniform plate thickness of 0.25 inches.

The third approximation values of p and q, equations (54) and (67) are now substituted into equations (27') and (28'), and the residuals calculated for a variety of hub rotations (ϕ = 0.05, 0.10, 0.15, 0.20, 0.25, 0.30, 0.35, 0.40, 0.45 and 0.50 radians). The residuals were all "small" as shown by the sample table (see Table I). The small residuals indicate that the third approximation solutions for p and q, equations (54) and (67), are quite close to the exact solutions.

Using the program shown in Appendix I, based on the third approximation values of p and q, equations (54) and (67); the loading parameter ϕ was calculated (recall this is related to the torque associated with a given hub rotation, and should remain constant from the hub to the outside edge of the plate). The loading parameter, ϕ, remained constant to four decimal places for all hub rotations (again, see Table I).

The program was also implemented to calculate the radial displacement, u, and the transverse displacement, v. Sample values are shown in Table I and curves are presented showing the variation of u and v as a function of radial distance for certain values of hub rotation, ϕ, in figures (4) and (5).

TABLE I

A SAMPLE TABLE OF THE COMPUTER RESULTS FOR A HUB ROTATION OF 0.30 RADIANS

r	p_3	q_3	ϕ	RF*	RS*	u	v
1.00000	0.045699	0.29550	0.012168	9.53×10^{-6}	-2.57×10^{-7}	0.045699	0.29550
1.05409	0.044179	0.26408	0.012169	1.09×10^{-5}	-1.54×10^{-7}	0.046569	0.27837
1.11803	0.041861	0.23289	0.012169	1.19×10^{-5}	-8.08×10^{-8}	0.046803	0.26038
1.19523	0.038772	0.20188	0.012169	1.24×10^{-5}	-3.34×10^{-8}	0.046341	0.24129
1.29099	0.034931	0.17103	0.012169	1.24×10^{-5}	-6.45×10^{-9}	0.045096	0.22080
1.41421	0.030355	0.14031	0.012169	1.19×10^{-5}	$+5.68\times10^{-9}$	0.042929	0.19843
1.58114	0.025054	0.10970	0.012169	1.08×10^{-5}	$+8.31\times10^{-9}$	0.039614	0.17345
1.82574	0.019033	0.07917	0.012169	9.05×10^{-6}	$+6.13\times10^{-9}$	0.034750	0.14454
2.23607	0.012293	0.04869	0.012169	6.70×10^{-6}	$+2.80\times10^{-9}$	0.027489	0.10888
3.16228	0.004830	0.01826	0.012169	3.65×10^{-6}	$+5.66\times10^{-10}$	0.015272	0.05773
5.00000	0.000000	0.00000	0.012169	1.46×10^{-6}	-3.25×10^{-14}	0.000000	0.00000

* RF and RS are the residuals of equations (27') and (28'), respectively, when the third approximation solutions for p and q are substituted for p and q in the equations.

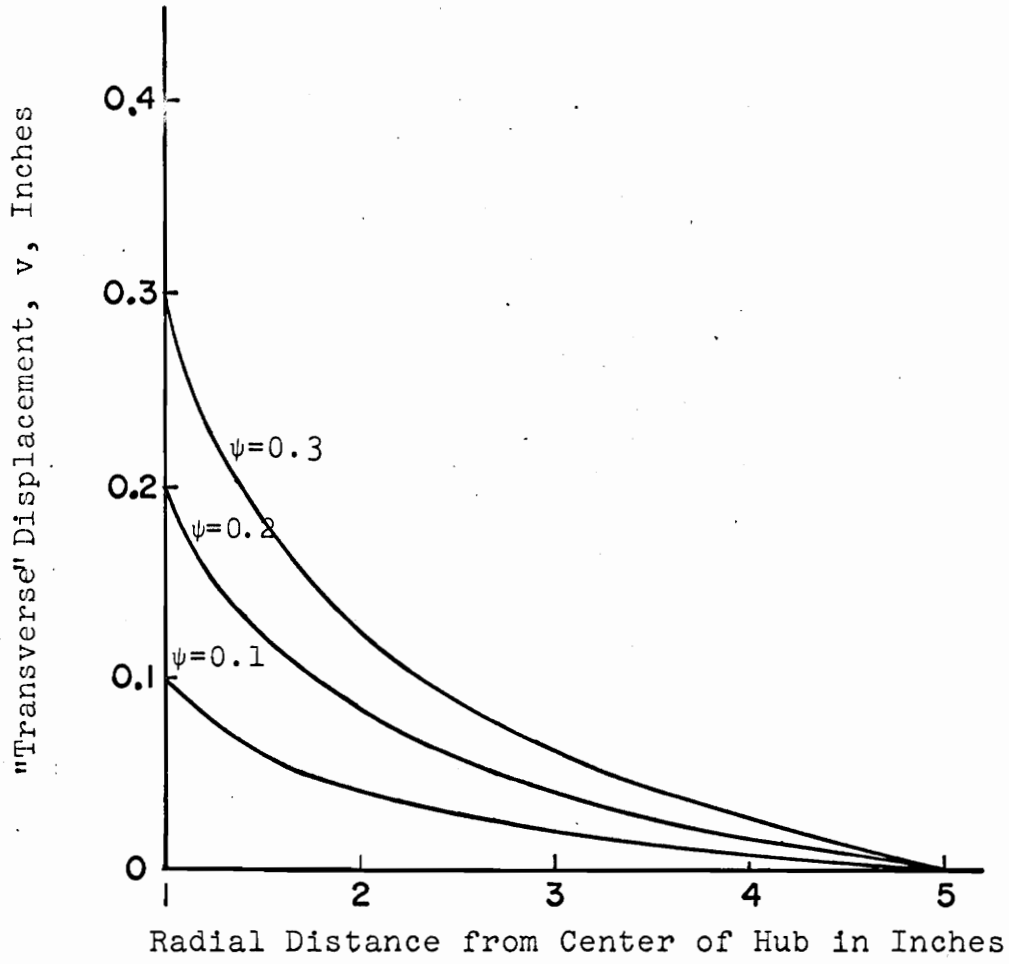

FIGURE 4

THE "TRANSVERSE" DISPLACEMENT, v, AS A FUNCTION OF RADIAL DISTANCE FOR THREE VALUES OF HUB ROTATION

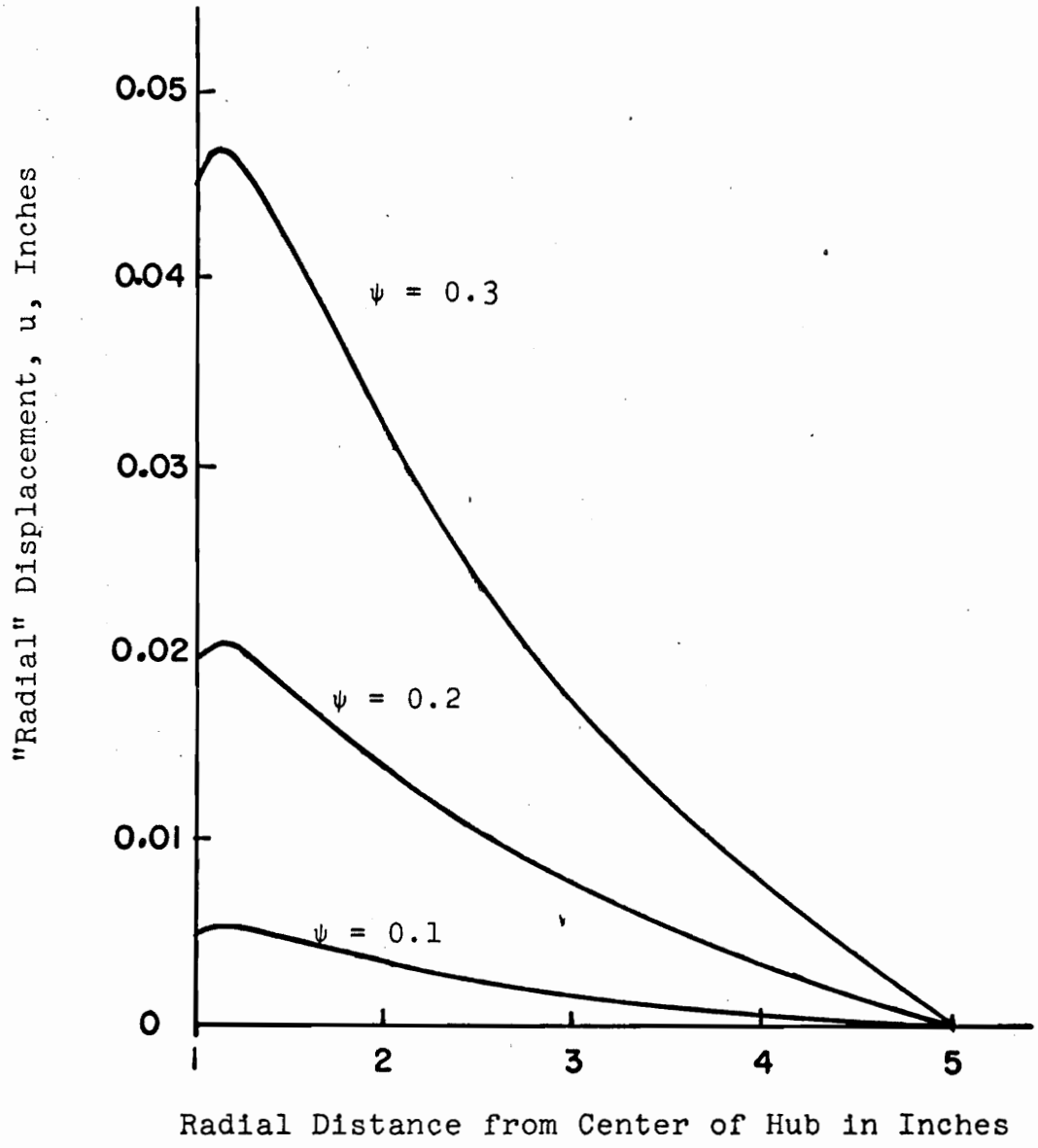

FIGURE 5

THE "RADIAL" DISPLACEMENT, u, AS A FUNCTION OF RADIAL DISTANCE FOR THREE VALUES OF HUB ROTATION

G.) INTERPRETATION OF RESULTS:

Usually, it is more convenient to visualize normal strain as the stretching of base vectors and shearing strain as the rotation of base vectors. In addition, the displacement gradients are assumed to be small. In the linear theory the Eulerian components of the strain tensor are equal to the Lagrangian components of the strain tensor, and the diagonal elements of the array are considered to be the normal strains and the off-diagonal terms are considered to be the shearing strains.

In the nonlinear case where the displacement gradients are not small, the Eulerian nonlinear components of the strain tensor cannot be simply interpreted as the stretching and rotation of base vectors. The problem we must now face is how to convert the components of the Eulerian nonlinear strain tensor into the entities which will agree with our fundamental concepts of normal and shearing strain. This problem is easily resolved in the following manner.

Recall that we deformed the body and then erected an orthogonal polar coordinate system in the deformed body. Let ds_i be the length of an infinitesimal line element along the coordinate axis θ^i after deformation and $(ds_i)_o$ be the length of the infinitesimal line element before

deformation. We may then write: (In the following development the summation convention is suspended.)

$$ds_i = \sqrt{G_{ii}}\, d\theta^i \tag{75}$$

and

$$(ds_i)_o = \sqrt{g_{ii}}\, d\theta^i \tag{76}$$

In equations (75) and (76), G_{ii} and g_{ii} are the components of the metric tensor in the deformed and the undeformed body, respectively.

Defining the normal strain in the conventional manner yields:

$$\epsilon_{ii} = \frac{ds_i - (ds_i)_o}{(ds_i)_o} \tag{77}$$

or equivalently, using equations (75) and (76):

$$\epsilon_{ii} = \sqrt{\frac{G_{ii}}{g_{ii}}} - 1 \tag{78}$$

where ϵ_{ii} are the normal strain components associated with the conventional definition of normal strain.

Utilizing a basic statement of the Eulerian nonlinear strain tensor (see Green and Zerna[6], page 57) we write:

$$2\, E_{ij} = G_{ij} - g_{ij} \tag{79}$$

Appropriately substituting equation (79) into equation (78) will yield:

$$\epsilon_{ii} = \sqrt{1 + \frac{2\, E_{ii}}{g_{ii}}} - 1 \tag{80}$$

or

$$\epsilon_{11} = \frac{1}{\sqrt{1 - \frac{2\,E_{11}}{G_{11}}}} - 1 \tag{81}$$

In equations (80) and (81), E_{11} are the "normal"* components of the Eulerian, nonlinear strain tensor.

Let us now define the shearing strain in the conventional manner:

$$\epsilon_{ij} = \tan\,(\alpha_{ij} - \beta_{ij}) \tag{82}$$

where ϵ_{ij} are the shearing strain components associated with the conventional definition of shearing strain, α_{ij} is the angle between $\vec{g}_i$ and $\vec{g}_j$ and β_{ij} is the angle between $\vec{G}_i$ and $\vec{G}_j$. In our particular case, $\beta_{ij} = \pi/2$; thus we may write:

$$\cos\,\alpha_{ij} = \frac{g_{ij}}{\sqrt{g_{ii}\,g_{jj}}} \tag{83}$$

or using equation (79) and recalling $G_{ij} = 0$ if $\beta_{ij} = \pi/2$ we write:

$$\cos\,\alpha_{ij} = \frac{-2\,E_{ij}}{\sqrt{G_{ii} - 2\,E_{ii}}\sqrt{G_{jj} - 2\,E_{jj}}} \tag{84}$$

---

* In the future, when we write "normal" or "shearing" we will mean those components of the Eulerian, nonlinear strain tensor that are analogous to the normal and shearing components of the linear strain tensor. However, bear in mind these are not normal or shearing strains in the conventional sense.

Using a simple trigonometric identity, we can write from equation (83):

$$\sin \alpha_{ij} = \frac{\sqrt{g_{ii}\, g_{jj} - (g_{ij})^2}}{\sqrt{g_{ii}\, g_{jj}}} \tag{85}$$

Recalling the basic definition of shearing strain, equation (82), and the fact that $g_{ij} = \pi/2$ we write:

$$\epsilon_{ij} = \tan\left(\alpha_{ij} - \frac{\pi}{2}\right) = -\cot \alpha_{ij} \tag{86}$$

Substituting equations (84) and (85) into (86) yields:

$$\epsilon_{ij} = \frac{-g_{ij}}{\sqrt{g_{ii}\, g_{jj} - (g_{ij})^2}} \tag{87}$$

or equivalently

$$\epsilon_{ij} = \frac{2 E_{ij}}{\sqrt{(G_{ii} - 2 E_{ii})(G_{jj} - 2 E_{jj}) - 4(E_{ij})^2}} \tag{88}$$

Equations (81) and (88) express the relationships between the conventional normal and shearing strains and the "normal" and "shearing" strains of the Eulerian non-linear strain tensor.

In our particular case we may write:

$$\epsilon_{rr} = \frac{1}{\sqrt{1 - 2 E_{rr}}} - 1 \tag{89}$$

$$\epsilon_{\theta\theta} = \frac{1}{\sqrt{1 - 2 E_{\theta\theta}}} - 1 \tag{90}$$

$$\epsilon_{r\theta} = \frac{2 E_{r\theta}}{\sqrt{(1 - 2 E_{rr})(1 - 2 E_{\theta\theta}) - 4(E_{r\theta})^2}} \tag{91}$$

Examination of equations (81) and (88) indicate that if the strains are small the normal and shearing strains defined in the conventional manner are equal to the "normal" and "shearing" strains of the Eulerian nonlinear strain tensor.

The relationship between the normal strain as conventionally defined and the "normal" strain of the Eulerian nonlinear strain tensor is very easy to obtain. Using either equation (89) or (90), assign a value to the "normal" Eulerian nonlinear strain and calculate the conventional normal strain. If this is done the curve shown in Figure 6 is the result.

Now consider a uniaxial state of stress. Recall that we assumed the components of the stress tensor were linearly related to their corresponding components of the Eulerian nonlinear strain tensor. This assumption is shown in Figure 7 as a straight solid line. We must now interpret this relationship in terms of the conventional definition of strain. Figure 6 represents the relationship between the "normal" Eulerian nonlinear strain and the conventional normal strain; consequently, if we convert the abscissa of Figure 7 from the "normal" Eulerian nonlinear strain to the conventional normal strain by means of Figure 6 the curved, dashed line of Figure 7 results. The

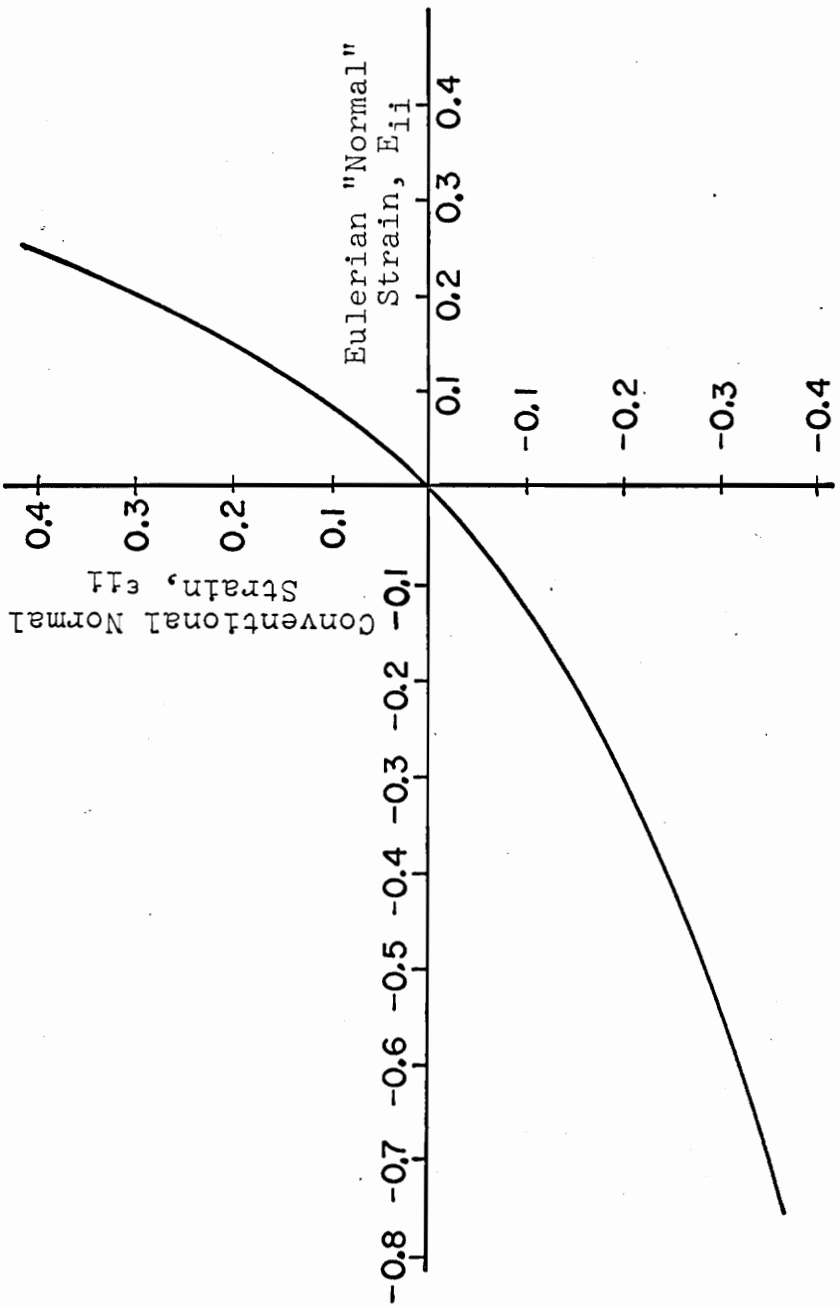

FIGURE 6

THE RELATIONSHIP BETWEEN THE CONVENTIONAL NORMAL STRAIN AND THE EULERIAN "NORMAL" STRAIN

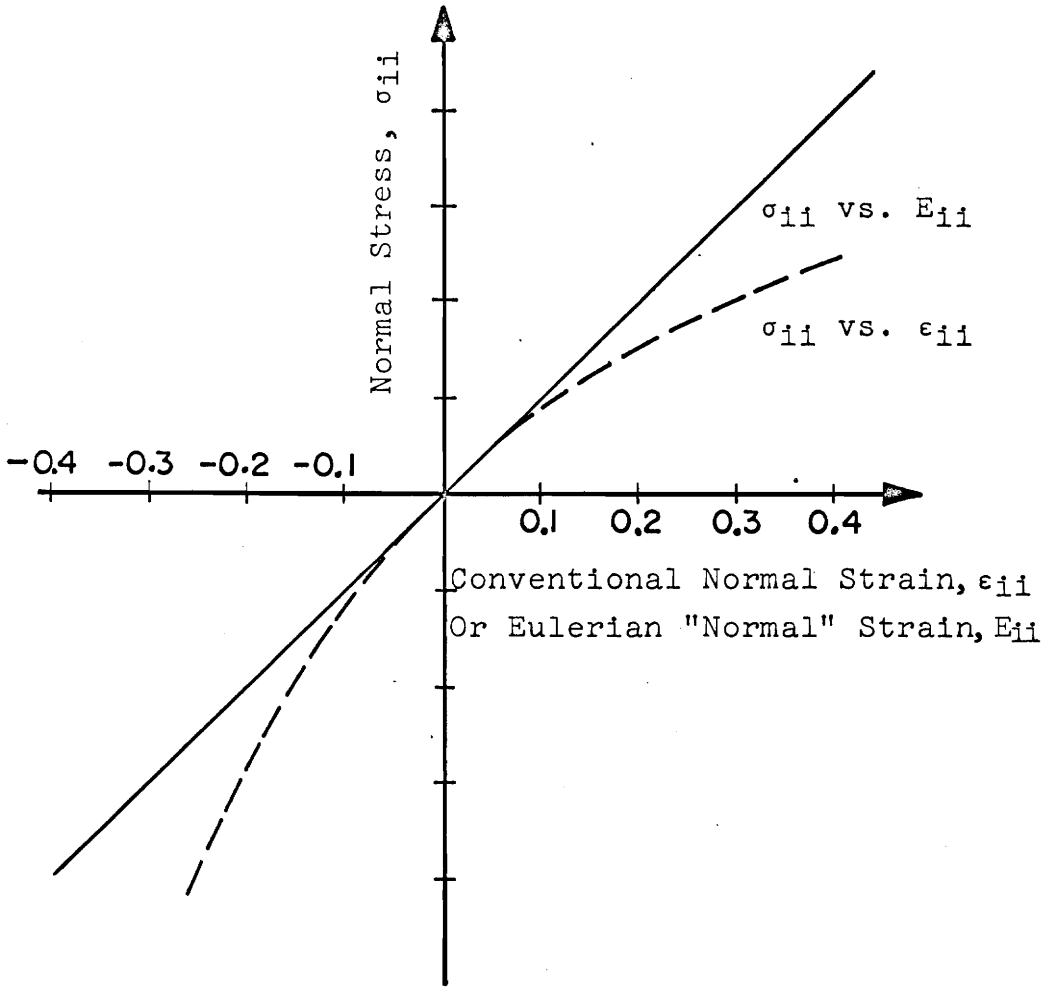

FIGURE 7

A HYPOTHETICAL, CONVENTIONAL, NORMAL STRESS-STRAIN CURVE DEVELOPED WITH THE FINITE STRAIN THEORY

curved, dashed line of Figure 7, then, represents the conventional stress-strain curve for the case of uniaxial stress (compression and tension).

Let us now consider a state of shearing stress. The state of shearing stress we will consider is the response of an element of the elastomeric, circular plate subjected to a finite rotation of its hub. The element of the plate we will consider is adjacent to the hub. A question may arise concerning why a state of pure shear is not considered. This is, in some respects, a moot question; but, primarily, a state of pure shear was not considered because a pure shear specimen is not used to determine the shearing modulus of elastomeric materials. Furthermore, the experimental specimen used to determine the shearing modulus of an elastomer is similar to an element of the plate. Using the computer results, E_{rr}, $E_{r\theta}$ and $E_{\theta\theta}$ were calculated using equations (5), (6) and (7). These results were then substituted into equation (91), and the relationship between the conventional shearing strain and the "shearing" strain of the Eulerian nonlinear strain tensor for the element of the plate were obtained. This relationship is shown in Figure 8. Bear in mind this is not the pure shear relationship. It was also assumed that a linear relationship existed between the shearing stress and the "shearing"

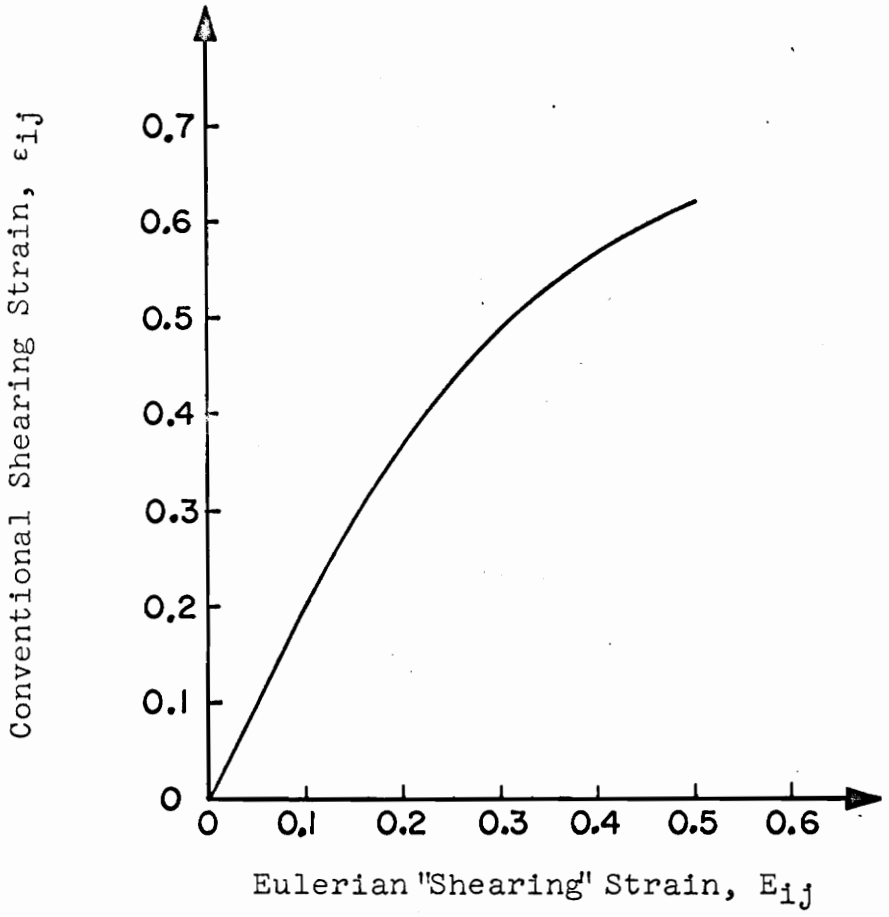

FIGURE 8

RELATIONSHIP BETWEEN CONVENTIONAL SHEARING STRAIN AND THE EULERIAN "SHEARING" STRAIN

strain component of the Eulerian nonlinear strain tensor; this assumption is shown as a solid straight line in Figure 9. Again, if the abscissa coordinate of the solid straight line is converted from the Eulerian "shearing" strain to the conventional shearing strain as indicated in Figure 8, a conventional stress-strain curve results. The conventional shearing stress-strain curve is shown as the dashed, curved line of Figure 9. Again bear in mind this is not a pure shear stress-strain curve. A little reflection will indicate that this has little, if any, effect upon the value of the infinitesimal shearing modulus.

Figure 10 displays the conventional shearing strain and the "shearing" strain of the Eulerian nonlinear strain tensor at the hub of the elastomeric, circular plate as a function of the plate rotation.

Figure 11 shows the variation of the loading parameter given by equation (73) as a function of the hub rotation of the plate.

To compare experiment and theory, we must relate the plate loading parameter, ϕ (equation (73)), to the applied experimental torque. The only unknown in the plate loading parameter is G, the infinitesimal shearing modulus. Once G is determined, the loading parameter can be converted to applied torque very easily. Figure 12 is the torque-angle

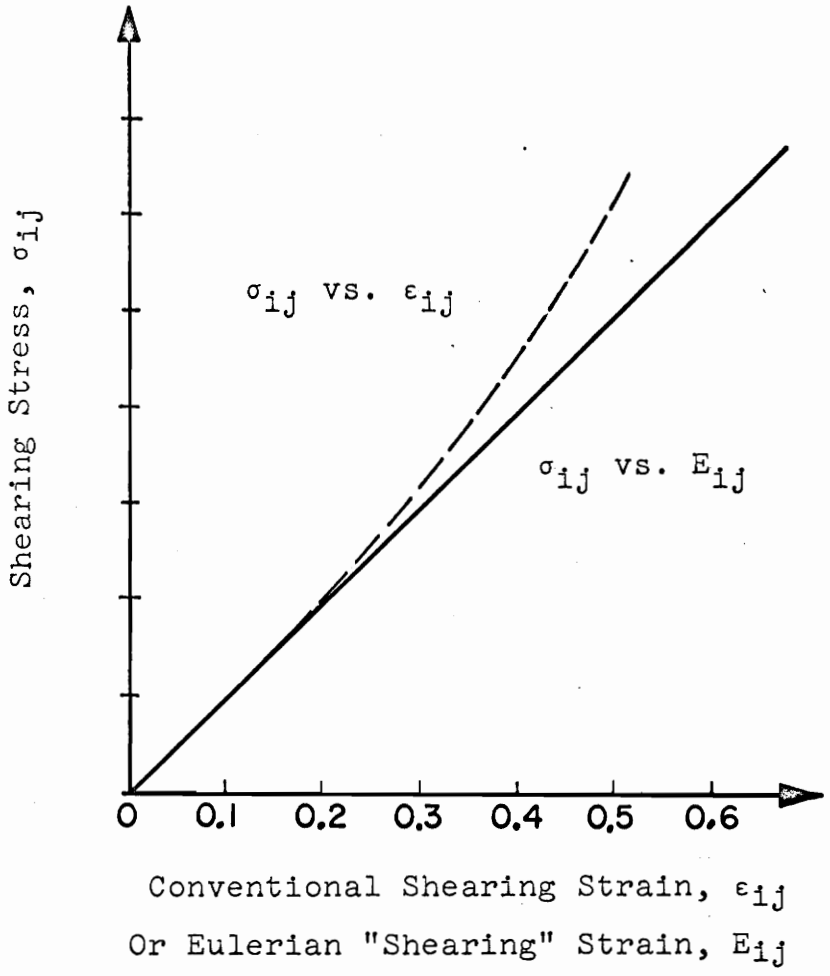

FIGURE 9

A HYPOTHETICAL CONVENTIONAL SHEARING STRESS-STRAIN CURVE DEVELOPED WITH THE FINITE STRAIN THEORY

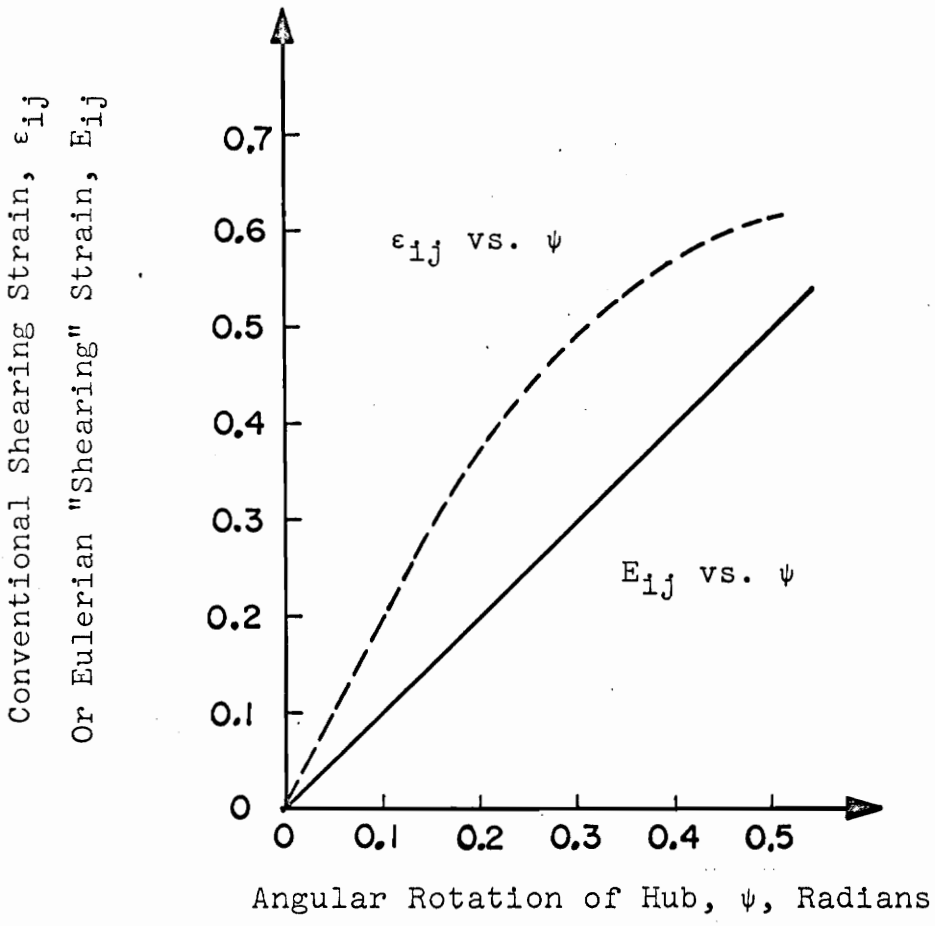

FIGURE 10

THE VARIATION OF SHEARING STRAIN AT THE HUB OF THE HUBBED, CIRCULAR PLATE DUE TO THE ANGULAR ROTATION OF THE HUB

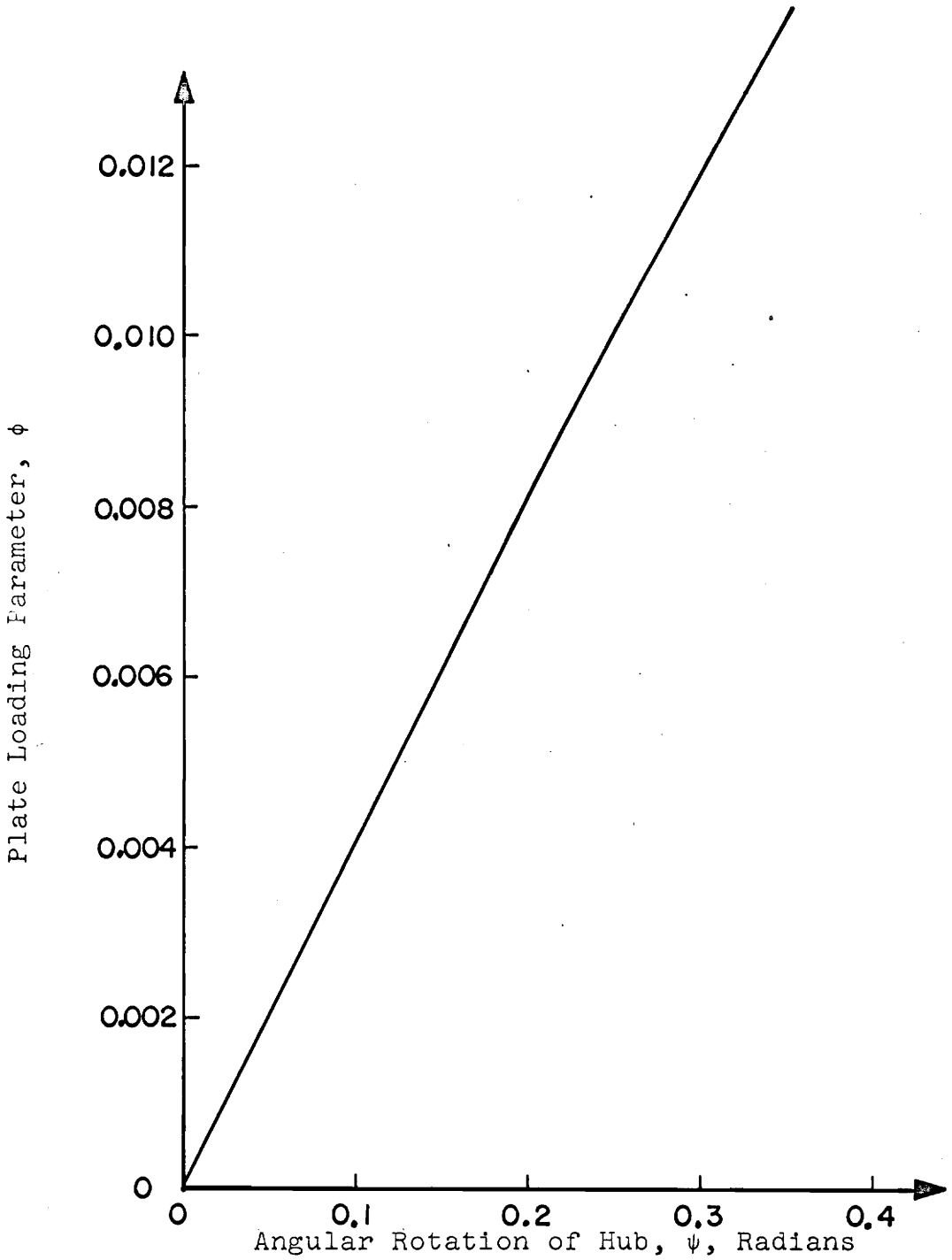

FIGURE 11

VARIATION OF THE LOADING PARAMETER DUE TO ANGULAR ROTATION OF THE HUB OF THE HUBBED, CIRCULAR PLATE

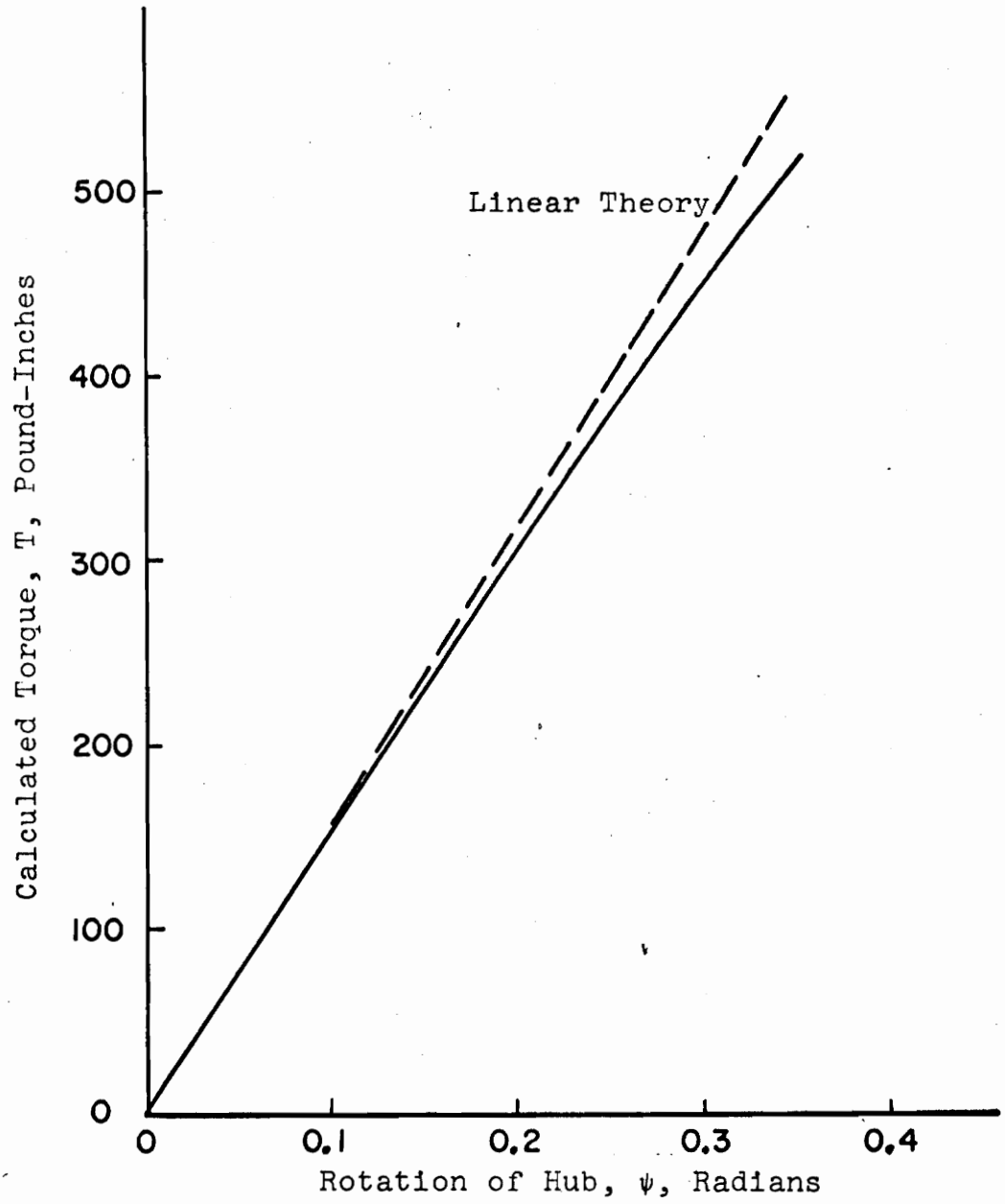

FIGURE 12

THE RELATIONSHIP BETWEEN TORQUE AND HUB ROTATION AS PREDICTED BY THE SOLUTION OF THE GOVERNING EQUATIONS

of hub rotation relationship as given by the theoretical analysis using the infinitesimal shearing modulus of the plate material. The manner in which the infinitesimal shearing modulus, G, was determined will be discussed in the experimental section of this thesis.

IV. THE EXPERIMENTAL INVESTIGATION

A.) OBJECT:

The object of the following simple experiments was twofold: first, to verify the agreement of the proposed theory with experiment; and, secondly, to evaluate the material properties of the elastomer from which the hubbed, circular plate was cast. A simple, uniaxial compression experiment was performed to check the validity of the theory for compression. A uniaxial tensile test was performed to check the validity of the theory for tension; and, also, to evaluate the infinitesimal elastic modulus. A shearing experiment was also run to check the applicability of the theory to the shearing case and to evaluate the infinitesimal shearing modulus. Finally, a prototype of the clamped, hubbed, circular plate was tested to determine the accuracy with which the proposed theory would solve a specific problem.

B.) THE ELASTOMER:

All specimens used in the experiments were open cast of polyurethane. Castable polyurethane is an amine cured, polyether prepolymer; it possesses excellent birefringent properties (see Figure 2) and its stiffness is completely controllable by the addition of dioctylphthalate.

The tensile specimen, the shearing specimen and the prototype circular plate had the following composition:

Adiprene L	100 parts
Moca	11 parts
Dioctylphthalate	25 parts

The compression specimen was of unknown composition.

C.) A UNIAXIAL COMPRESSION TEST:

1.) The Specimen:

A cylindrical specimen was open cast of polyurethane (see Figure 13). The specimen was 0.973 inches in diameter and 1.472 inches long.

2.) The Experimental Set-Up:

The ends of the cylindrical test specimen were well lubricated with graphite and oil. The specimen was then placed between the heads of an MTS testing machine. (The MTS testing machine is a completely automatic testing machine whose functions are completely controllable from a remote console. The MTS machine has an integral X-Y plotter for the presentation of data.)

3.) The Experiment:

The movable head of the MTS testing machine was brought into contact with the cylindrical specimen; the head speed was set at 0.5 inches per minute and the limit switch was set for 0.5 inches of head travel. The machine was started; and, automatically, the specimen was loaded until the movable head had travelled 0.5 inches: then, automatically, the specimen was unloaded until the movable head returned to its starting position. The experimental data was presented as a force-deflection plot on the X-Y plotter.

The specimen was cycled three times as described above.

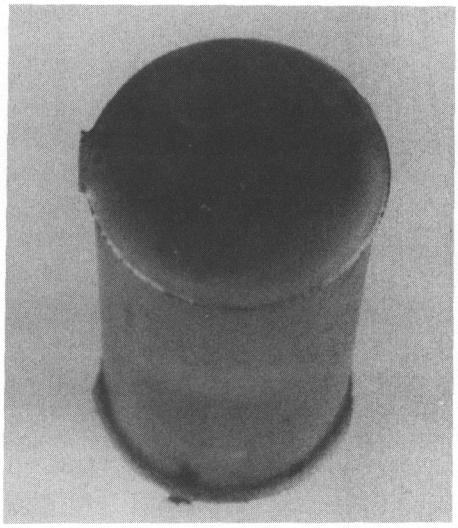

FIGURE 13: THE CYLINDRICAL, UNIAXIAL COMPRESSION SPECIMEN

Polyurethane exhibits a very high modulus on its first loading cycle due to polymer cross-linking. On the second and all subsequent loading cycles, the modulus is reduced from the first loading cycle. The load-deflection data is essentially invariant for all loading cycles after the first. Consequently, the experimental data of the third cycle was considered to be indicative of the material response to uniaxial compression.

D.) A UNIAXIAL TENSION TEST:

1.) The Specimen:

The uniaxial tensile specimens are shown in Figure 14. These specimens were cut from a cast sheet of polyurethane. The specimens were checked with a hand polarizer for residual stresses which might have been introduced in cutting the specimens, but no residual stresses were found. The specimens were six inches in overall length. The test section, located in the central portion of the dumbbell section, was one inch long, 0.5 inches wide and 0.122 inches thick.

2.) The Experimental Set-Up:

The specimen was placed in the air-actuated grips of a floor mounted INSTRON testing machine. (An INSTRON testing machine is a completely automatic testing machine whose functions are controllable from an integral control panel. The INSTRON machine has an integral X-Y plotter for the presentation of data.) An INSTRON extensometer was secured to the central one inch portion of the dumbbell section. The extensometer output was fed to the X-Y plotter as Y. The load was X input to the plotter.

3.) The Experiment:

The INSTRON machine was set to give a head velocity of 0.2 inches per minute and a chart speed of 0.5 inches

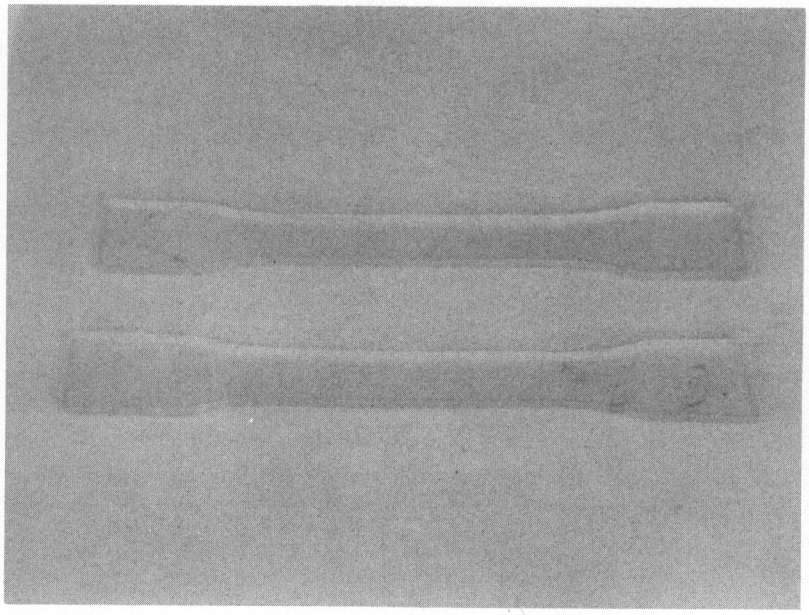

FIGURE 14: THE UNIAXIAL TENSILE SPECIMENS

per minute. The machine was started and the experiment was run until the one inch test section was deformed to a length of 1.5 inches. The specimen was unloaded, removed, reinserted and the experiment was rerun. The experiment was repeated three times with the third run being used for experimental data.

E.) TORSION OF THE PLATE:

1.) The Specimen:

An experimental plate of 5.5 inches outside radius, one inch inside radius and 0.25 inches thick was open cast of polyurethane. A one inch radius aluminum hub was integrally bonded to the inside circumference of the plate.

2.) The Experimental Set-Up:

The specimen was secured in a supporting jig of two aluminum plates; each aluminum plate had a ten inch diameter hole cut in its center and was faced 0.125 inches to a diameter of 11.25 inches. The specimen was then cemented on both sides over an area extending from a five inch radius to the outside edge; it was then positioned between the aluminum plates in contact with the facings of the aluminum plates. The plates were then bolted together; however, the spacing between the plates was shimmed in such a way that the plates did not compress the specimen. (The entire support of the specimen at its outer edge was due to the cement.) The central hub of the plate was drilled and broached such that a torque could be transmitted from a 0.5 inch diameter shaft through a key to the plate. The shaft transmitting the torque was supported on each side of the plate in polished holes. The complete experimental set-up is shown in Figure 15; assuming the plate is located

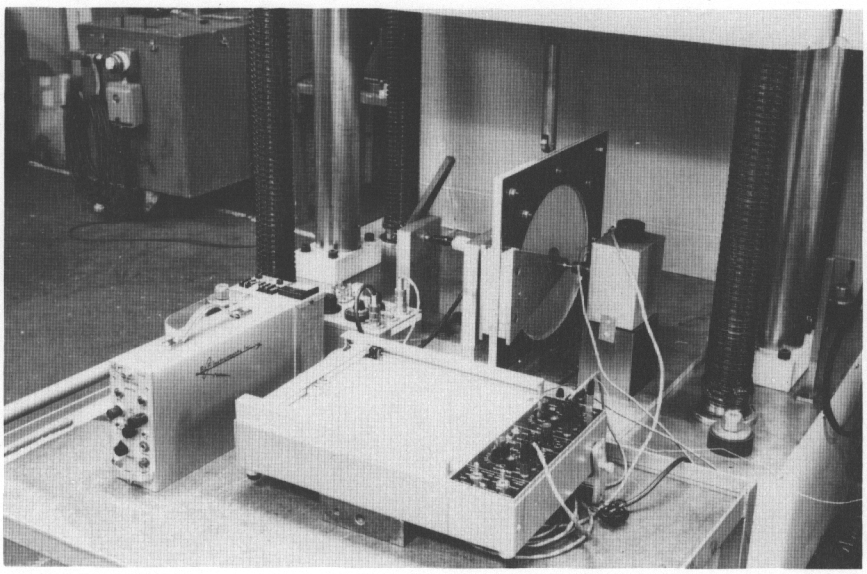

FIGURE 15 EXPERIMENTAL SET-UP FOR THE PLATE TORSION TEST

at 12 o'clock, the complete experimental set-up is as follows:

a.) 12 o'clock - the plate secured in its jig.

b.) 1 o'clock - a precision potentiometer which was used to measure the angular rotation of the torque input shaft (the central hub of the plate).

c.) 11 o'clock - a torque gage, actually a 3/8 inch drive socket extension which was strain gaged and calibrated to indicate torque. The torque gage was supported at each end in nylon bushings in vertical support plates, it was connected to the load shaft of the plate by a 3/8 inch drive universal joint and was loaded by a vertical force applied to an arm. (See right hand side of Figure 16.)

d.) 10 o'clock - a bridge box connected to the torque gage, a DC voltage supply, and a recorder.

e.) 8 o'clock - a DC voltage supply connected to the bridge box.

f.) 6 o'clock - a "Moseley" X-Y plotter recording

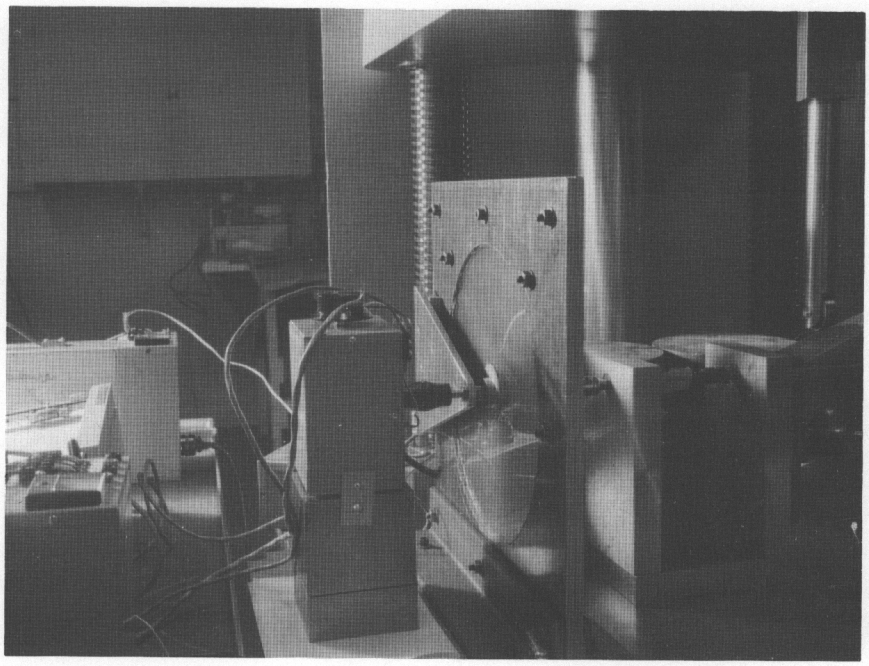

FIGURE 16 PLATE TORSION EXPERIMENTAL SET-UP IN POSITION FOR TEST (Note Load Application Method at Right Side of Photo.)

torque gage output as the Y signal and the precision potentiometer output as the X signal.

A battery is used as the DC input to the precision potentiometer.

A schematic of the plate torsion experimental set-up is shown in Appendix II.

3.) The Experiment:

Three plates were tested in torsion at various times during February and March 1965. The first experiment was unsuccessful due to a bond failure between the plate and the central hub; the second experiment was also unsuccessful due to incomplete data collection before the ultimate failure of the plate. The third experiment was considered successful; it was conducted in the following manner:

a.) The specimen was instrumented as previously discussed and was placed in a Tinius Olsen Universal Test Machine as shown in Figure 16. (It should be mentioned that the Tinius Olsen Test Machine was used only as a test vehicle - no data was taken from the machine.)

b.) The loading device (a rigid bar with a ball bearing end) was brought into contact with the loading arm at an eccentricity of five inches. The plate

containing the experimental fixture was wedged to prevent translation on the weighing table and weighted to prevent possible overturning of the fixture.

c.) The loading head was adjusted to yield a loading rate of 0.2 inches/minute and the test was started.

d.) Several runs were made in the following order:

i. one run to a 10° rotation of the hub

ii. three runs to a 20° rotation of the hub

iii. one run to a 25° rotation of the hub

iv. one run to ultimate failure of the plate.

Figures 17, 18 and 19 have no direct bearing on the present investigation, but are included to indicate the nature of the response of a clamped, hubbed, elastomeric circular plate to a large axi-symmetric rotation of the hub.

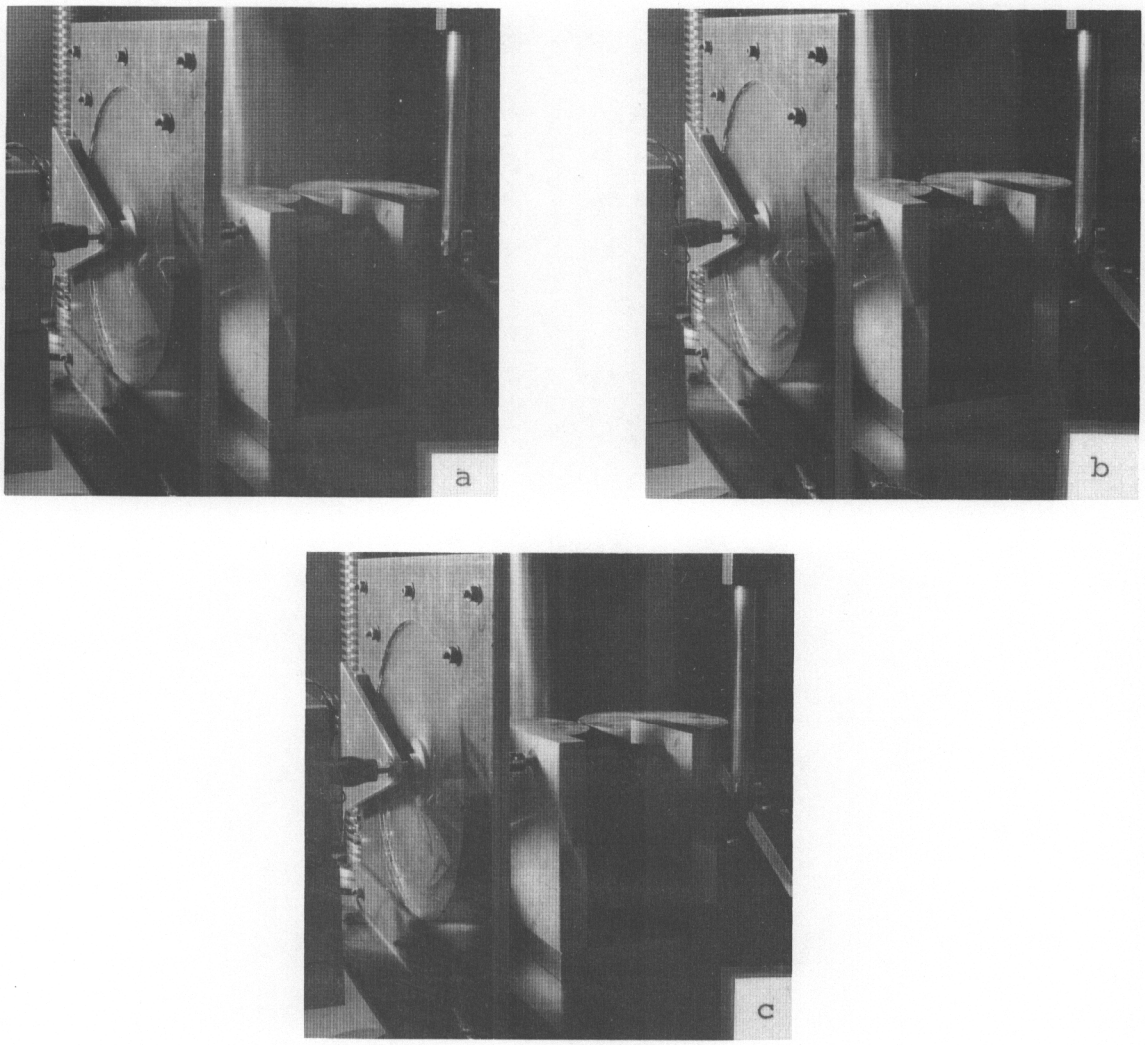

FIGURE 17 PROGRESSIVE BUCKLING OF PLATE DUE TO TORSION.
(Note shadows at 6 o'clock on the plate)

a) Approximately 31 Degree Rotation of Hub
b) Approximately 34 Degree Rotation of Hub
c) Approximately 36 Degree Rotation of Hub

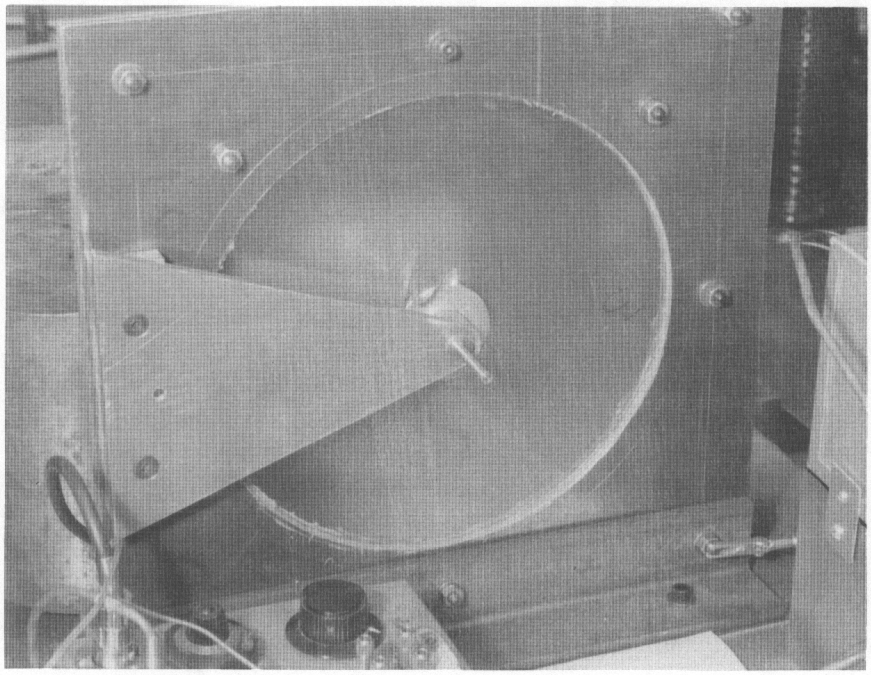

FIGURE 18 THE PLATE AFTER ULTIMATE FAILURE

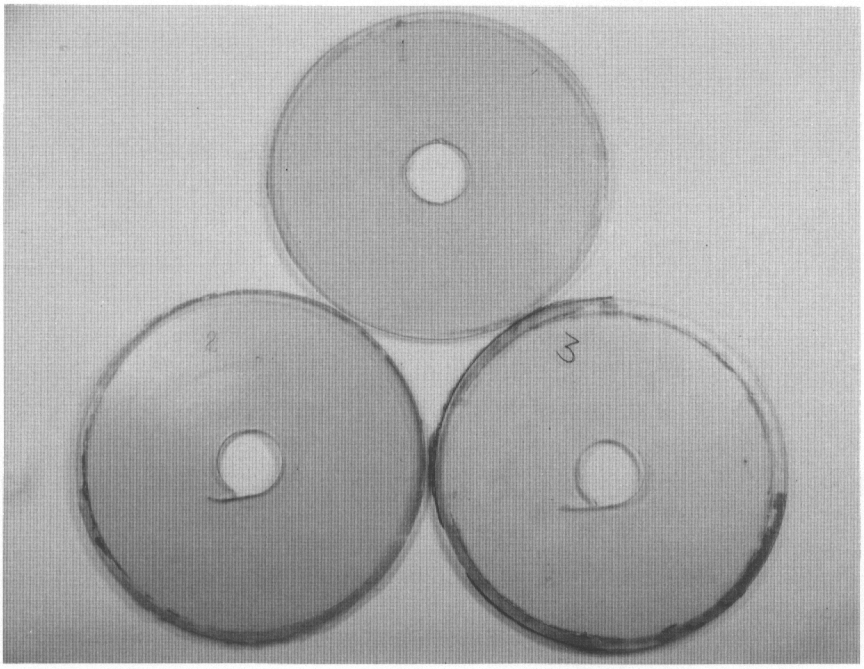

FIGURE 19 THREE PLATES AFTER FAILURE (Note Numbers on Plates).

Plate 1 Bond Failure
Plate 2 Buckling-Tension Failure
Plate 3 Buckling-Tension Failure

F.) THE SHEARING EXPERIMENT:

1.) The Specimen:

The experimental shearing specimen is shown in Figure 20. The specimen is the standard Lord D-837 shearing specimen; its dimensions (on each side of the central load transfer plate) are 0.882 inches long, 0.5 inches deep and 0.5 inches wide.

2.) The Experimental Set-Up:

The specimen was secured in the testing jig as shown in Figure 21. The testing jig was then placed in a Tinius Olsen Universal Testing Machine as shown in Figure 22. Figure 22 shows the complete experimental set-up for the determination of the shearing response of the specimen. In Figure 22 the testing jig is placed on a 0-1000 pound Lebow load cell, a DC voltage supply is connected to the load cell and the load cell output is taken to the Y axis of the Moseley X-Y plotter. The displacement of the specimen is determined by means of a Tinius Olsen deflectometer (an LVDT) used in conjunction with an ATC. The ATC output is taken to the X axis of the Moseley X-Y plotter. A schematic of the shearing modulus experiment is shown in Appendix III.

3.) The Experiment:

The specimen was placed in the Tinius Olsen Universal

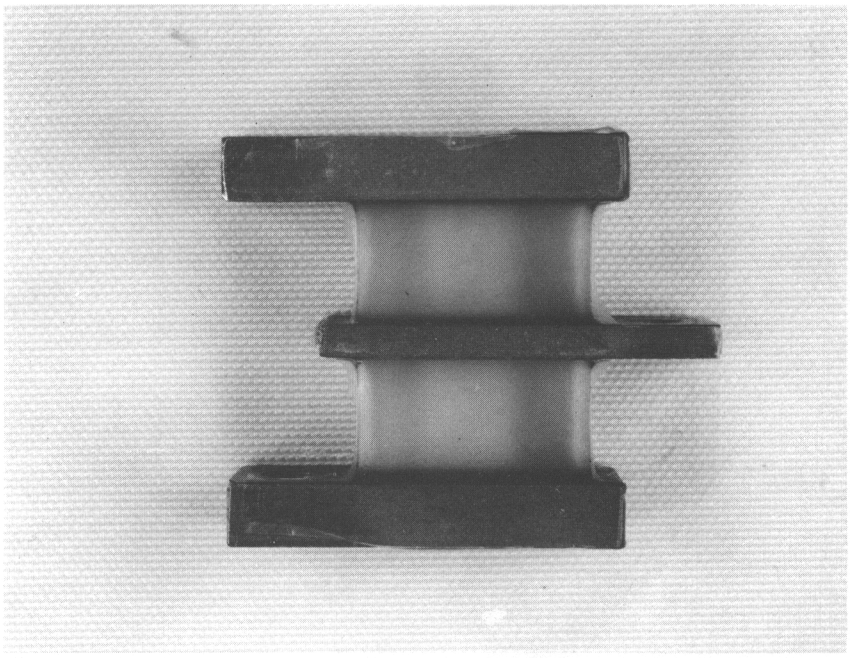

FIGURE 20 THE SHEARING MODULUS EXPERIMENTAL SPECIMEN

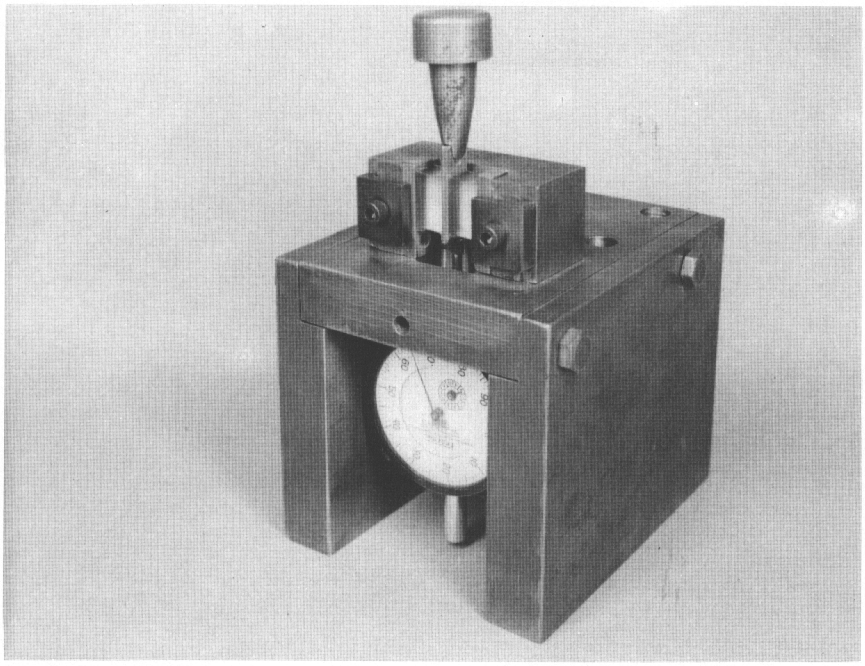

FIGURE 21 THE SHEARING MODULUS EXPERIMENTAL SPECIMEN IN TESTING JIG

Testing Machine as shown in Figure 22. (Again, the Tinius Olsen Testing Machine is used only as a test vehicle.) The loading head was brought into contact with the load transfer head of the testing jig, and the experiment was begun. The specimen was tested through three cycles of deflection to 0.2 inches over a variety of loading rates varying from 0.015 inches/minute to 0.833 inches/minute. In all cases the response of the specimen was very nearly constant indicating a lack of strain rate sensitivity.

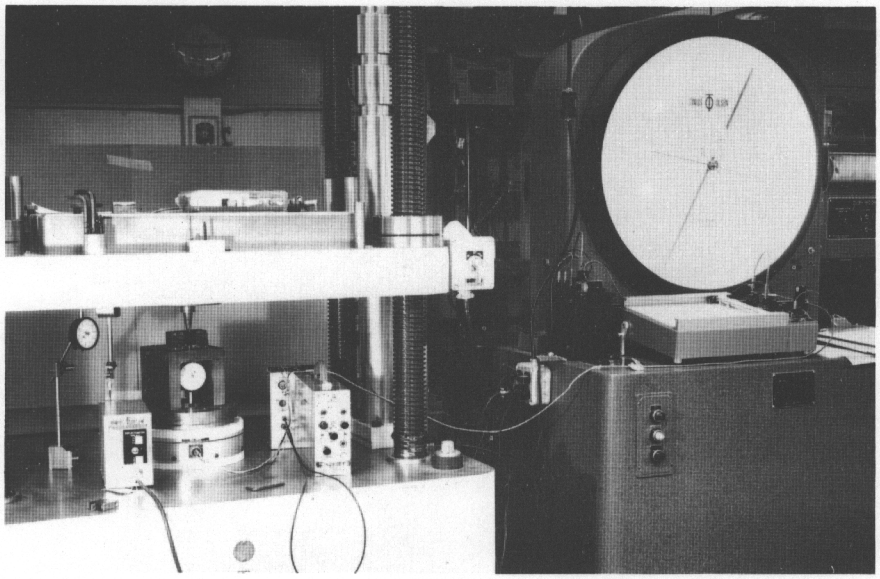

FIGURE 22 DETERMINATION OF SHEARING MODULUS; EXPERIMENTAL SET-UP

G.) THE EXPERIMENTAL RESULTS:

The corrected results of the uniaxial compression experiment are shown by the solid line in Figure 23. The correction that is made on the raw experimental data is to correct the stress for the change of the cross sectional area due to the large strain imposed on the specimen. The correction is based on an incompressibility assumption.

The data obtained in the uniaxial tension experiment is displayed in corrected form by the solid line of Figure 24. The same correction is applied here as in the uniaxial compression case. From the corrected data, the infinitesimal elastic modulus was determined to be 1492 psi. Note the correction applied to the raw data does not affect the value of the infinitesimal elastic modulus.

Recall that the compression specimen and the tensile specimen were of different compositions. Consequently, it will be impossible to obtain a continuous stress-strain curve embracing both compression and tension. However, a plethora of experimental results in the rubber and elastomeric literature indicate that the infinitesimal tensile and compressive moduli are equivalent. For example, see Treloar[18].

A portion of a typical result of the plate torsion experiments is shown by the solid line of Figure 25. The

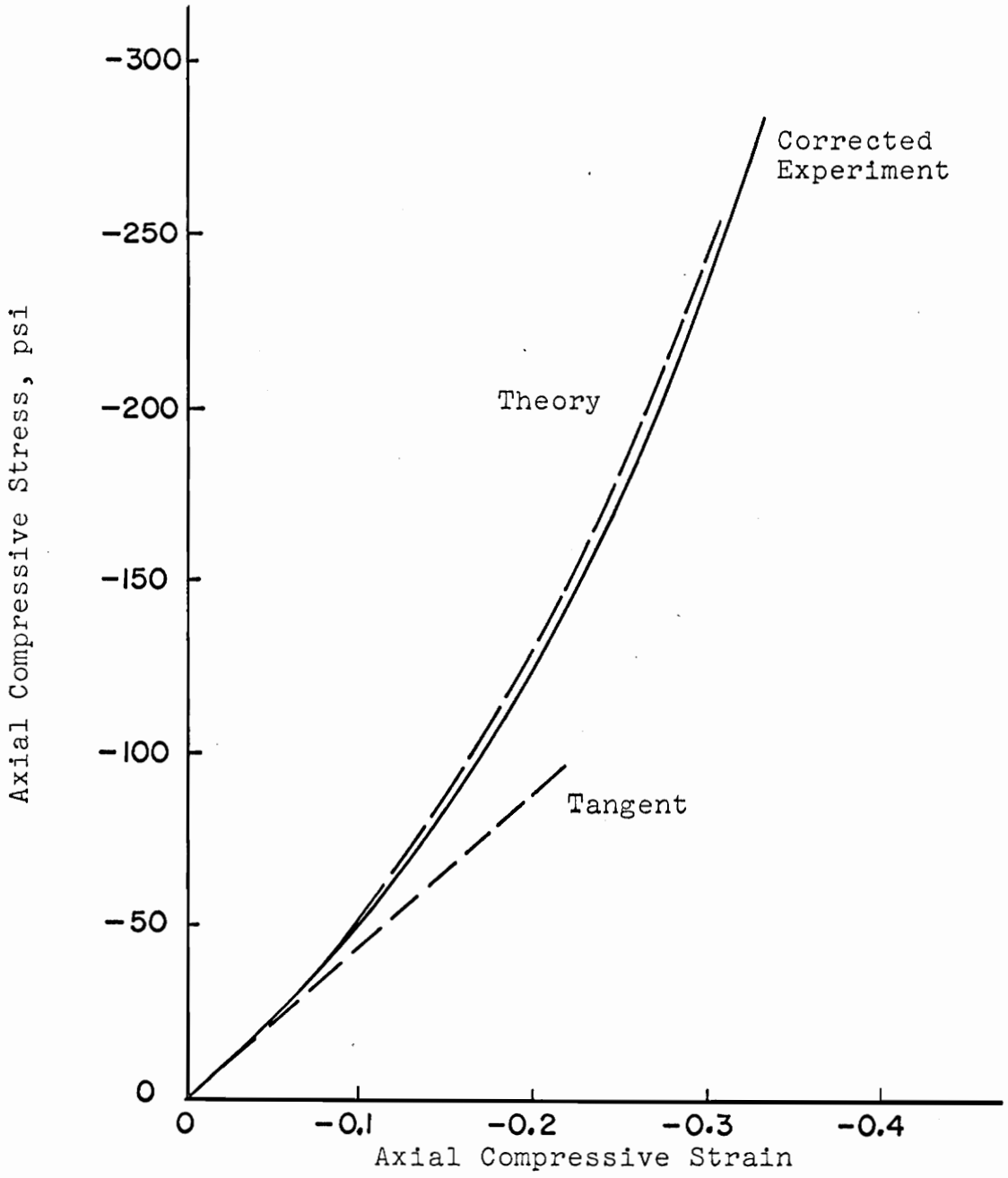

FIGURE 23

RELATIONSHIP BETWEEN THE CONVENTIONAL, UNIAXIAL, COMPRESSIVE NORMAL STRESS AND STRAIN AS DETERMINED BY EXPERIMENT AND AS PREDICTED BY THE FINITE STRAIN THEORY

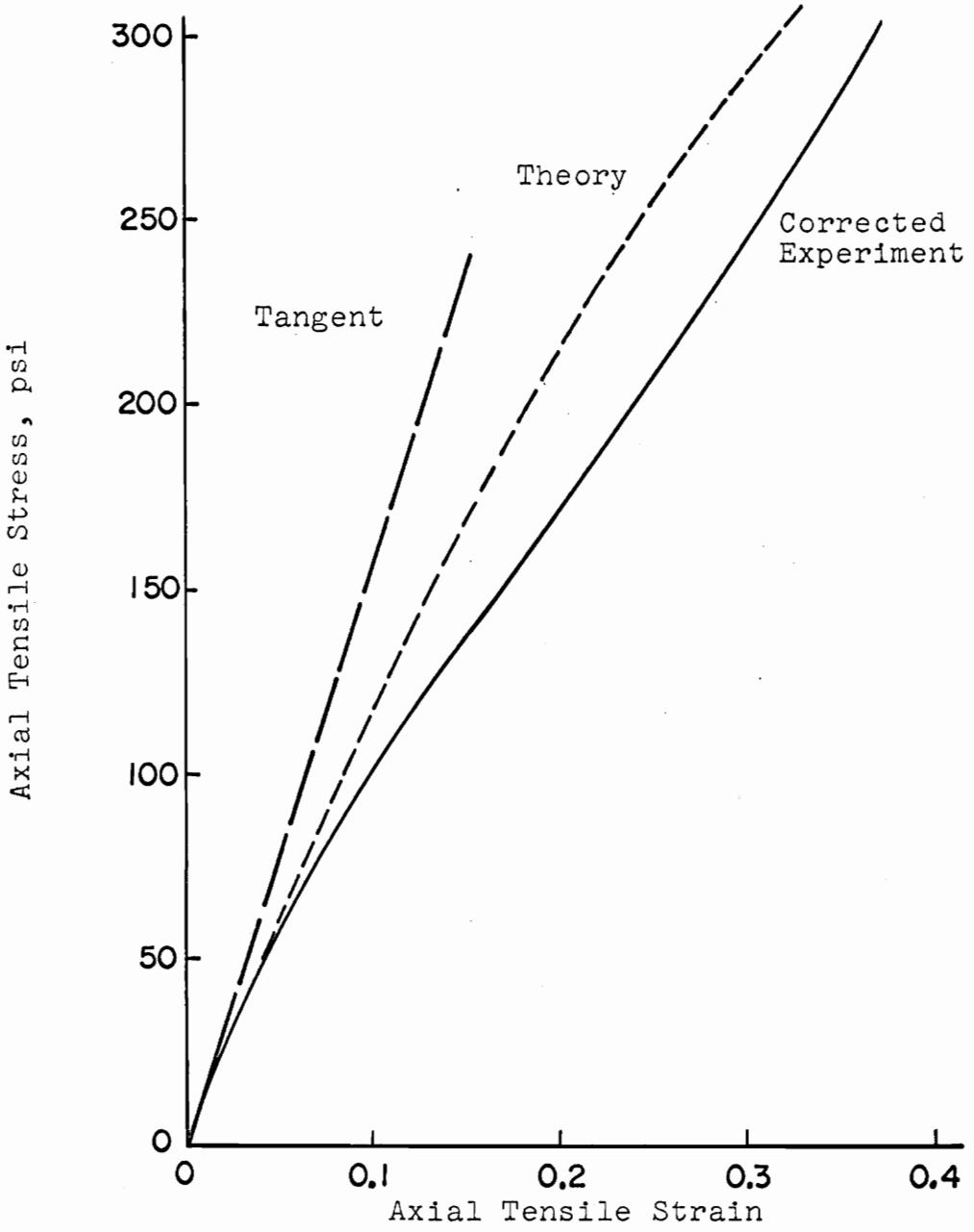

FIGURE 24

RELATIONSHIP BETWEEN THE CONVENTIONAL, UNIAXIAL, TENSILE NORMAL STRESS AND STRAIN AS DETERMINED BY EXPERIMENT AND AS PREDICTED BY THE FINITE STRAIN THEORY

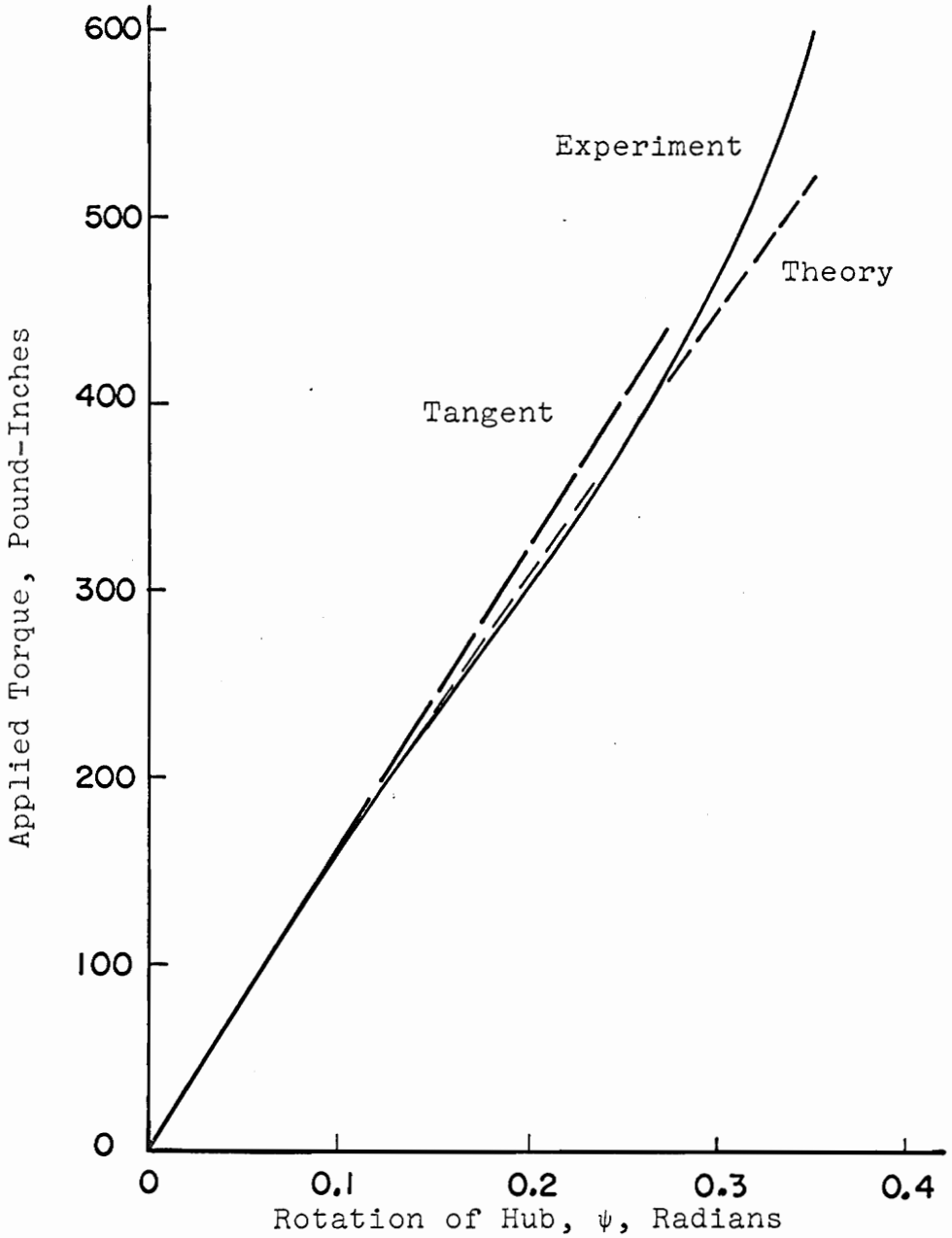

FIGURE 25

THE TORQUE, ANGULAR ROTATION OF HUB RELATIONSHIP FOR THE HUBBED, CIRCULAR PLATE SUBJECTED TO AXISYMMETRIC TORQUE AS DETERMINED BY EXPERIMENT AND AS PREDICTED BY THE FINITE STRAIN THEORY

curve presented is from the data of the 0 to 25° rotation of the hub experiment (run iii).

The data collected in the shearing phase of the experimental work is presented in Figure 26 as a solid line. These results indicated that the infinitesimal shearing modulus of the polyurethane specimen was 481.5 psi.

Using the values of the infinitesimal elastic and infinitesimal shearing moduli, the linear equation relating the two moduli yields a value of 0.54 for Poisson's ratio.*

The buckling process of the experimental plate is not being considered in this investigation; but, nonetheless, it was observed and was quite interesting. When the rigid central hub had been rotated through about 31 degrees, two small "dimples" appeared on the plate. The dimples were diametrically opposed at about 6 and 12 o'clock on the plate (Figure 17), and were concave. As the angular rotation was increased, the dimples became deeper; the deepening was accompanied by a very slow clockwise undulation. (The load was being applied in the clockwise direction.) When the buckling torque was reached (rapid decay of

---

* The value of 0.54 for Poisson's ratio is assumed to be due to experimental error. Reports in the literature indicate that the value of Poisson's ratio for polyurethane is 0.5.

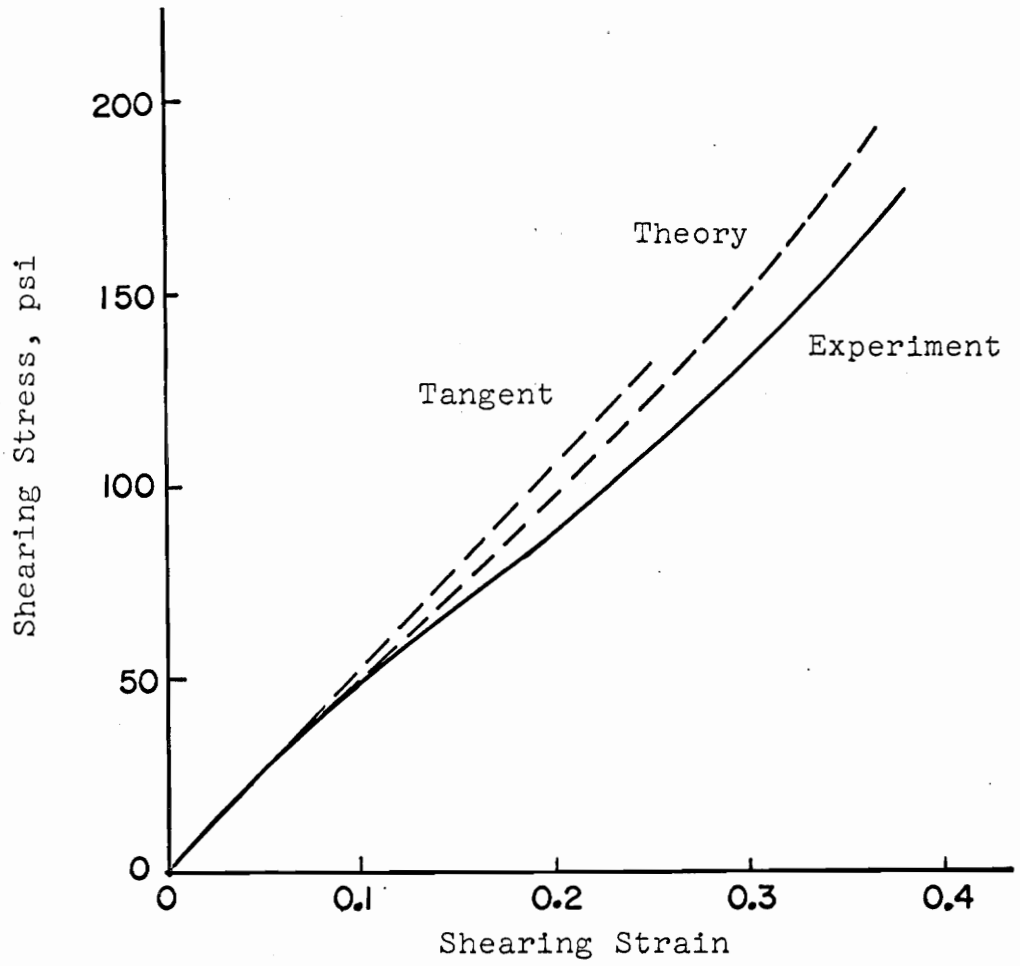

FIGURE 26

RELATIONSHIP BETWEEN CONVENTIONAL SHEARING STRESS AND STRAIN AS DETERMINED BY EXPERIMENT AND AS PREDICTED BY THE FINITE STRAIN THEORY

torque); two, well-defined, diametrically opposed buckles appeared. These two buckles extended about one inch from the hub; and, as the angular rotation increased, these buckles extended toward the outer edge of the plate accompanied by "wrinkling" on the clockwise side of the buckles. The buckles never reached the outer edge of the plate. At an angular rotation of the hub of about 56^{0} to 57^{0}, an apparent tensile failure occurred followed immediately by a bond failure. It was noted that the buckles were neither tangent nor radial to the central hub. Stein and Hedgepeth[13] report this fact as a result of their work with a hubbed membrane subjected to an axi-symmetric torque.

V. SUMMARY AND CONCLUSIONS

In this thesis, a finite strain theory was proposed. Furthermore, it was demonstrated that conventional stress-strain relations can be developed from the theoretical analysis (section III.G). Consequently, the proposed theory can be compared to actual experiment for several loading situations; and, thus, the validity of the proposed theory can be evaluated.

First, let us consider the application of the theory to the finite strain, uniaxial compression case. The corrected experimental results are shown in Figure 23 by the solid curved line. To apply the theory, draw a tangent to the "infinitesimal" portion of the corrected experimental curve as shown in Figure 23. This, of course, corresponds to the statement of the finite strain theory; if the abscissa is considered to be the Eulerian "normal" compressive strain. To compare the corrected experimental results with the finite strain theory one must convert the abscissa of the finite strain theory (the line tangent to the infinitesimal portion of the corrected experimental curve) from the Eulerian "normal" compressive strain to the conventional compressive strain. This is easily accomplished by using Figure 6. When this conversion from the Eulerian "normal" compressive strain to the conventional normal compressive strain is performed the finite strain theory

curve, as labeled in Figure 23, results. Comparing theory and experiment for the uniaxial compressive case, it is seen that the agreement, qualitatively and quantitatively, is extremely good up to strain levels of 30 percent.

Secondly, consider the case of uniaxial tension. The corrected results of the uniaxial tension experiment are shown in Figure 24 by the solid, curved line. Again, draw a line tangent to the infinitesimal portion of the corrected experimental curve (as before, this represents the statement of the finite strain theory if the abscissa is considered to be the "normal" Eulerian tensile strain). The Eulerian "normal" tensile strain must, again, be converted to the conventional normal tensile strain before experiment and theory may be compared. This is easily accomplished by using Figure 6. When the finite strain theory for the tensile case is converted to conventional coordinates the curved, dashed line of Figure 24 is the result. The agreement of theory and experiment is qualitatively "good" up to strain levels in the range of 20 to 25 percent. Above strain levels of about 25 percent, the theory and the experiment diverge. This was as expected as some elastomeric materials, including polyurethane, undergo a physical change at certain strain levels. This physical change is essentially a crystallization phenomenon wherein the polymer changes to

a crystalline structure. This change is usually indicated by a change in color of the specimen (for polyurethane).

Now, consider the shearing case. In the shearing case, we are confronted by a dilemma at the onset, as the shearing specimen (Figure 20) is not a true shearing specimen for finite deformation because of the two free edges. This problem could be resolved by theoretically analyzing the shearing specimen. Unfortunately, this has not been done for the finite deformation case. Let us, then, use the results of the plate torsion analysis. An element near the central hub of the plate torsion specimen should behave similarly to the shearing modulus specimen. Note, we said similarly as an element in the plate can or will be subjected to two normal strains as there are no free edges in the plane of the plate whereas in the shearing modulus specimen (Figure 20) there are two free edges. Hence the energy level of the element in the plate should be higher than an element in the shearing modulus specimen for the same "shear" deformation. It should be noted the shearing specimen dilemma has been appreciated for several years, but little work has been done to alleviate the problem. As far as is known (to the author) no one has tried to analyze the shearing specimen, and the only paper that has been published concerning possible corrections was published

several years ago by Read[17].

Nonetheless, to compare the finite strain theory with the shearing experiment; the following approach was used. Using the results of the plate torsion analysis and experiment, the relationship between the conventional shearing strain and the Eulerian "shearing" strain was calculated using the results of section III.G. This relationship is shown in Figure 8. Using the results of the shearing modulus experiment, the infinitesimal shearing modulus was determined. (Note that the two free edges of the shearing modulus specimen should not appreciably affect the determination of the infinitesimal shearing modulus.) Using the value of the infinitesimal shearing modulus the finite strain theory is shown as the straight, dashed line of Figure 26 where the abscissa values corresponding to this curve are understood to be Eulerian "shearing" strain. Then using Figure 8, the Eulerian, "shearing" strain is converted to conventional shearing strain; and the finite strain theory for shear is shown as the dashed, curved line of Figure 26. The shearing modulus experimental data is shown in Figure 26 as the curved, solid line. At this point, the agreement between theory and experiment is "good," but recall our argument concerning the two free edges of the shearing modulus specimen. If we were to

restrain the two free edges of the shearing modulus specimen, the energy level of the specimen would be increased. This would move the experimental curve of Figure 26 upward toward the theoretical curve of Figure 26. In addition, the effect upon the energy level of restraining the two free edges of the shearing modulus specimen would be negligible for small strains, and the effect would, of course, for the larger strains become more profound. Thus, it is believed that the finite strain theory is also applicable to the shearing case with sufficient accuracy to warrant engineering consideration.

To further study the applicability of the finite strain theory, the problem of the response of a clamped, hubbed, circular elastomeric plate subjected to a finite, axi-symmetric rotation of the hub was studied. This problem will demonstrate the applicability of the finite strain theory to the solution of a realistic engineering problem. An approximate solution was obtained by hand and then extended by means of a digital computer as explained in section III.F.

This solution was based upon the assumption that Poisson's ratio of the material was 0.5; by experiment, Poisson's ratio was determined to be 0.54. This, of course, is an eight percent error; but the effect of this

error is not too profound if one checks the terms in equations (27) and (28) that contain Poisson's ratio. The complete solution of the plate-torsion problem is not determined until the infinitesimal shearing modulus is known; however, the infinitesimal shearing modulus is now known to be 481.5 psi as the result of the shearing modulus experiment. Consequently, a solution of the plate-torsion problem is completed and this solution is presented as a torque-angle of hub rotation plot in Figure 12 as a curved, solid line and in Figure 25 as a dashed, curved line. The experimental torque-angle of hub rotation relationship is shown in Figure 25 as a curved, solid line.

The agreement between the finite strain theory and the experiment for the axi-symmetric rotation of the hub of a hubbed, clamped, elastomeric circular plate is excellent up to a hub rotation of about 0.27 radians. For values of hub rotation greater than about 0.27 radians the theory and experiment diverge.

The divergence of the theoretical and experimental results for hub rotations greater than about 0.27 radians is easily explained. Recall that the results of the tension experiment when compared to theory also indicated this type of divergence; and, in addition, recall the statement made by Gubkin[15] which is cited in the Introduction:

"...In view of this, the principal stresses are equal in value, but opposite in sign."

Thus, there is always a tensile principal stress in the plate; which, when the value becomes large enough will develop a condition of crystallinity which alters the physical properties of the elastomer. Evidentally, the tensile stress developed in the plate becomes the predominating factor in the response mechanism at a hub rotation of 0.25 to 0.30 radians. This is somewhat substantiated by the failure of the plate as shown in Figure 19. Thus, it must be stated that the finite strain theory breaks down in the presence of tensile stresses which are of sufficient magnitude to alter the physical properties of the elastomer. However, in general, this is not an insurmountable problem as there are elastomers which can sustain very high strain levels before the physical properties are altered.

In conclusion, the finite strain theory has been proved to be adequate for the engineering analysis of certain finite strain problems. The theory is in excellent agreement with the uniaxial compression, finite strain problem. The theory appears to be in agreement with the shearing response of elastomeric materials subjected to finite shears. However, it is believed that additional work should be done to improve finite, shearing strain, experi-

mental techniques. The theory agrees, qualitatively, with experiment up to strain levels of 20 to 25 percent for the uniaxial, tensile finite strain case; but, admittedly this is the weakest case of the proposed theory. As previously indicated, certain elastomers have a tendency to change their physical properties at certain tensile strain levels. Consequently, if an elastomer with a much greater tolerance to tensile strain were used; the qualitative agreement between theory and experiment could be extended to much higher strain levels.

VI. ACKNOWLEDGMENTS

The author would like to express his appreciation to Dr. T. S. Chang and Dr. D. Frederick of the Virginia Polytechnic Institute for the advice and suggestions they offered in the writing of this thesis.

In particular, the author would like to express his grateful thanks to Dr. K. L. Cheng of the Lord Corporation for many hours of enlightening discussion concerning several important facets of this thesis.

In addition, thanks are due to Miss Patricia Podsiadlo for the splendid job she did in typing this work. Thanks are also extended to Mr. W. E. Benoit for preparing all the experimental samples.

In closing, the author would like to express his most heartfelt thanks to Prof. Dan H. Pletta -- who made it all possible.

VII. BIBLIOGRAPHY

1. Frederick, D. and Chang, T.S., Continuum Mechanics, Allyn and Bacon, Inc., Boston, 1965, page 79.

2. Rivlin, R.S., Large Elastic Deformations of Isotropic Materials, I. Fundamental Concepts, 1948, a. Phil. Trans. A, 240, pages 459-490.

3. Rivlin, R.S., Large Elastic Deformations of Isotropic Materials, II. Some Uniqueness Theorems for Pure Homogeneous Deformation, 1948, b. Phil. Trans. A, 240, pages 491-508.

4. Rivlin, R.S., Large Elastic Deformations of Isotropic Materials, III. Some Simple Problems in Polar Coordinates, 1948, c. Phil. Trans. A, 240, pages 509-525.

5. Love, A.E.H., A Treatise on the Mathematical Theory of Elasticity, Dover Publications, 1944.

6. Green, A.E. and Zerna, W., Theoretical Elasticity, Oxford: At The Clarendon Press, 1960.

7. Murnaghan, F.D., Finite Deformation of an Elastic Solid, John Wiley and Sons, 1951.

8. Mooney, M., A Theory of Large Elastic Deformation, Journal of Applied Physics, Vol. 11, September 1940, pages 582-592.

9. Carmichael, A.J. and Holdaway, H.W., Phenomenological Elastomechanical Behavior of Rubbers Over Wide Ranges of Strain, Journal of Applied Physics, Vol. 32, No. 2, February 1961, pages 159-166.

10. Carmichael, A.J. and Holdaway, H.W., Application of the Three Parameter Stress Function to Natural Rubbers of Widely Different Hardness, Journal of Applied Physics, Vol. 32, No. 9, September 1961, pages 1724-1728.

11. Timoshenko, S.P. and Goodier, J.N., Theory of Elasticity, McGraw-Hill, New York, 1951, pages 109-111.

12. Prescott, J., Applied Elasticity, Dover Publications, 1961, page 364.

13. Stein, M. and Hedgepeth, J.M., Analysis of Partly Wrinkled Membranes, NASA, TN D-813.

14. Mikulas, M., Behavior of a Flat Stretched Membrane Wrinkled by the Rotation of an Attached Hub, NASA, TN D-2456.

15. Gubkin, S.I. et al, Fotoplastichnost, Minsk, 1957, pages 70-75.

16. Sokolnikoff, I.S., Mathematical Theory of Elasticity, 2nd Ed., McGraw-Hill, New York, 1956.

17. Read, W.T., Effect of Stress-Free Edges in Plane Shear of a Flat Body, Journal of Applied Mechanics, December 1950, page 349.

18. Treloar, L.R.G., The Physics of Rubber Elasticity, Oxford: At The Clarendon Press, 2nd Ed. 1958, page 94.

VIII. VITA

The author was born January 24, 1930 in Clarendon, Pennsylvania. He attended elementary schools in Pennsylvania and New York and graduated from Cathedral Preparatory School, in Erie, Pennsylvania in June 1947. Immediately following graduation, he enlisted in the U.S.M.C. and served until September 1951. In September 1951, he entered the Virginia Polytechnic Institute and in June 1956 received a Bachelor of Science Degree in Mechanical Engineering. The author then entered the Graduate School at Virginia Polytechnic Institute as a teaching assistant; and in June 1958, he obtained a Master of Science Degree in Applied Mechanics. He then started work toward the Doctor of Philosophy Degree in Mechanics. In June 1959, the author resigned at the Virginia Polytechnic Institute and accepted a job with Marquardt Aircraft Company in Van Nuys, California as a Development Engineer. Due to government contract cancellations, the author left California and returned to the Virginia Polytechnic Institute as an Assistant Professor of Engineering Mechanics in January 1960, where he again started studying toward the Doctor of Philosophy Degree. In June 1963, the author again resigned at the Virginia Polytechnic Institute and accepted employment with the Lord Corporation in Erie, Pennsylvania. At present, the author

is a Senior Engineer in the Engineering Research Department of the Lord Corporation.

P. S. Healy

APPENDIX I

THE 1107 DIGITAL COMPUTER PROGRAM FOR THE EVALUATION OF THE THIRD APPROXIMATION SOLUTIONS AND THE RESIDUALS OF THE GOVERNING EQUATIONS FOR THE HUBBED,CIRCULAR, ELASTOMERIC PLATE. THE COMPUTER LANGUAGE IS ALGOL.

```
@ RUN 70014,5,(120,20)                    ##################################
@ ALG HEALY
COMMENT  PHI AND THE RESIDUALS OF THE GOVERNING EQUATIONS FOR THE
THIRD APPROXIMATION SOLUTIONS FOR P AND Q  $
FORMAT  HEAD (X8,'I',X8,'PT',X12,'QT',X12,'PHI',X12,'RF',X12,'RS',X12,
     'U',X12,'V',A1.1)  $
FORMAT  ANS (X5,I4,7(X2,R12.5),A1)  $
INTEGER I,J,N,O  $
REAL ARRAY A,B,C,D,G,DG,DDG,X,T,Z(0..96)  $
REAL R,S,K,H,Y,W,V,U,PT,DPT,DDPT,QT,DQT,DDQT,PHI,RF,RS,E,F  $
LOCAL LABEL  DONE  $
READ (K,H)  $
AGAIN..
READ ( DONE,R,S)  $
WRITE  ('R IS',R)  $
FOR I = (1,1,9) DO
     Z(I) = ((H**I)-1)/((H-1)**I)  $
COMMENT  CALCULATION OF CONSTANTS  $
     A(1) = R*(1+K*Z(2))  $
     A(2) = -(K*R)  $
     B(2) = -(K*S*R)/(H-1)  $
     B(3) = (1/3)*(K*S*R)  $
     B(1) = S-B(2)*Z(2)-B(3)*Z(3)  $
     C(2) = -0.5*K*(A(1)*A(1)+B(1)*B(1))
          -(A(1)*A(2)+B(1)*B(2))/(H-1)
               -(A(2)*A(2)+B(2)*B(2))/((H-1)**2)
                    -B(2)*B(3)/((H-1)**3)  $
     C(3) = -0.3333*(1+2*K)*(A(1)*A(2)+B(1)*B(2))
          +(B(1)*B(3)/(H-1))
               +(B(2)*B(3)/((H-1)**2))
                    +(B(2)*B(2)/((H-1)**3))  $
     C(4) = -0.1666*(3+2*K)*(A(2)*A(2)+B(2)*B(2))
          -0.50*(1+K)*B(1)*B(3)  $
     C(5) = -0.10*(7+3*K)*B(2)*B(3)  $
     C(6) = -0.10*(10+3*K)*B(3)*B(3)  $
     Y = 0  $
FOR I = (2,1,6) DO
     Y = Y+C(I)*Z(I)  $
     C(1) = R-Y  $
```

```
      W = 0  $
FOR I = (1,1,3) DO
      W = W + B(I)/((H-1)**I)  $
      B(0) = -W  $
      E = 0  $
FOR I = (1,1,6) DO
      E = E +C(I)/((H-1)**I)  $
      C(0) = -E  $
    D(2) = 0.50*(2*B(2)*C(0)-2*B(0)*C(2))  $
    D(3) = (1/6)*(2*B(2)*C(1)+6*B(3)*C(0)-2*B(1)*C(2)-6*B(0)*C(3))  $
    D(4) = (1/12)*(6*B(3)*C(1)-6*B(1)*C(3)-12*B(0)*C(4))  $
    D(5) = (1/20)*(4*B(3)*C(2)-4*B(2)*C(3)-20*B(0)*C(5)-12*B(1)*C(4)) $
    D(6) = (1/30)*(-10*B(2)*C(4)-30*B(0)*C(6)-20*B(1)*C(5))  $
    D(7) = (1/42)*(-18*B(2)*C(5)-6*B(3)*C(4)-30*B(1)*C(6))  $
    D(8) = (1/56)*(-28*B(2)*C(6)-14*B(3)*C(5))  $
    D(9) = (1/72)*(-24*B(3)*C(6))  $
      F = 0  $
FOR I = (2,1,9)  DO
      F = F + D(I)*Z(I)  $
      D(1) = S-F  $
WRITE (HEAD)  $
COMMENT  EVALUATION OF THE APPROXIMATIONS  $
FOR I=(0,1,96) DO BEGIN
      X(I) = 25-0.25*I  $
      T(I) = SQRT(H/X(I))  $
FOR J=(1,1,9) DO BEGIN
      G(J) = ((X(I)**J)-1)/((H-1)**J)  $
      DG(J) = J* (X(I)**(J-1))/((H-1)**J)  $
      DDG(J) = J*(J-1)* (X(I)**(J-2))/((H-1)**J)  $
END  $
      PT = 0  $
      DPT = 0  $
      DDPT  = 0  $
FOR N= (1,1,6) DO BEGIN
      PT = PT+C(N)*G(N)  $
      DPT = DPT +C(N)*DG(N)  $
      DDPT = DDPT+C(N)*DDG(N)  $
END  $
      QT = 0  $
      DQT = 0  $
DDQT = 0  $
FOR O=(1,1,9) DO BEGIN
      QT = QT+D(O)*G(O)  $
      DQT = DQT+D(O)*DG(O)  $
      DDQT = DDQT+D(O)*DDG(O)  $
END  $
      PHI = (1-PT)*DQT+QT*DPT  $
```

```
      RF= (1-2*X(I)*DPT-PT)*DDPT+K*DPT*DPT+(2*X(I)*DQT-QT)*DDQT
           +K*DQT*DQT  $
      RS = (1-PT)*DDQT+QT*DDPT  $
      U = T(I)*PT  $
      V = T(I)*QT  $
      WRITE  (ANS,I,PT,QT,PHI,RF,RS,U,V)  $



END  $
GO TO AGAIN  $
DONE..
@N XQT HEALY
0.75
25
0.0050      0.0998
0.0112      0.1494
0.0199      0.1987
0.0457      0.2955
0.0789      0.3894
@ EOF
@ FIN
```

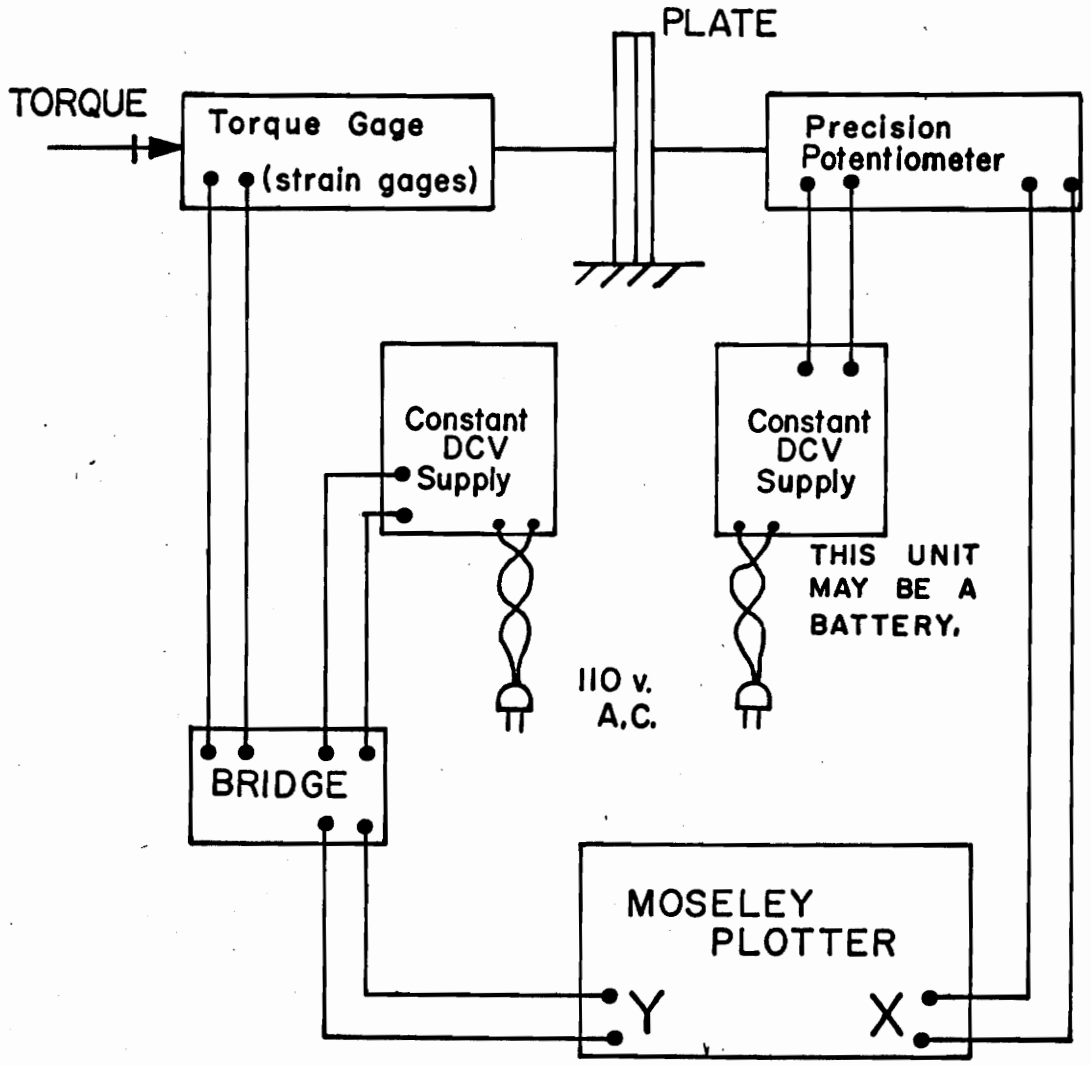

APPENDIX II

SCHEMATIC OF INSTRUMENTATION FOR

PLATE TORSION EXPERIMENT

A FINITE STRAIN THEORY, AND ITS APPLICATION TO THE PLANE STRESS RESPONSE OF POLYURETHANE

an

Abstract of a Thesis Presented by

G. S. HEALY

to the

Graduate Faculty

of the

Virginia Polytechnic Institute

in

Candidacy for the Degree of

DOCTOR OF PHILOSOPHY

in

Engineering Mechanics

May, 1966

A FINITE STRAIN THEORY, AND ITS APPLICATION TO THE PLANE STRESS RESPONSE OF POLYURETHANE

The theory proposed in this thesis is an attempt to bridge the gap that exists between the linear and nonlinear theories of Elasticity.

The theory is applied to the solution of a hubbed, clamped, circular plate made of polyurethane whose hub is subjected to a "large" axi-symmetric twist. This particular problem is attacked in the conventional manner of the generalized plane stress problem of linear elasticity. However, the strain displacement relations are formulated in the Eulerian manner and the displacement gradients are not assumed to be small. In addition, a more general stress-strain relationship than the conventional Hookean form is assumed.

The solution is checked by experiment; and in addition, three auxiliary problems; the uniaxial compression problem, the uniaxial tension problem, and a shear problem are checked experimentally to further check the validity of the proposed theory when applied to the finite strain response of polyurethane.